This document contains firstly a response to the reviewers, point by point, followed by the adjusted version of the manuscript with track changes showing.

Review 1

This is a neat paper, a very practical application of data and modeling efforts that the authors and others have been pursuing for years. The study reaches clear recommendations, which is especially gratifying.

We thank the reviewer for taking the time to read and review our paper. We are very pleased to hear their enthusiasm for the findings and recommendations.

Lines 183-184. This is not a complete sentence.

Thank you – now complete.

Clearly the near-surface dust concentration is especially important, and I know that CALIPSO sensitivity tends to diminish within the lowest 75 – 100 m of the surface. Is the reason that CAMS produces lower dose than CALIPSO for near-surface dust concentrations the assumption that the CALIPSO extinction at 100 m is extrapolated to the surface? The confidence with which you can assess the elevation of a near-surface concentration peak seem especially relevant based, e.g., on Figures 4c, 4e, 5c, and 5e, and it comes up again in the discussion of Figure 8. (I now see some discussion in lines 495-502. And I agree it is surprising in light of CALIOP being lower than other measurements. I'm wondering whether there is any EarliNet data that might help here.)

In terms of EARLINET sites, these cover Europe and therefore cannot be used to validate our profiles in this study. However, the suggestion of ground-based lidar validation is valuable. In fact this is the topic of ongoing research, and will be published separately in due course. We discuss the potential application of ground-based lidar data in the conclusion. As the reviewer points out we discuss these differences in the lowest portion of the vertical profile in the discussion. We have added a signposting sentence to the beginning to the results section so the reader knows the differences are discussed later on, "In this section we present the key results and findings of this work. A full discussion of the potential causes for differences between datasets is given in Section 5."

Section 2.3.3. I think you do as good a job as one can with available satellite data in constraining the dust mass concentration. But it might be worth also making some assessment of the uncertainty in mass concentration, e.g., associated with the uncertainty in the MEC. (I realize you compare the model and two lidar estimates with each other, which might represent a rough estimation of uncertainty due to s in Equation 1, but I think you are using the same MEC to obtain concentrations for all three.) (Again, I now see you say a bit more about MEC uncertainty in lines 503-513. Ok, so is the recommendation that we need better measurements of dust MEC?)

Yes, we certainly agree that we need better measurement constraints on dust MEC. Additional text has been added to the conclusions to emphasize this, "(particularly mass extinction coefficient, which is a crucial property in relating model-calculated mass loading to satellite-derived optical retrievals)."

Further, is there any available data on actual engine wear, that might be used to test or constrain the overall results?

The simple answer to the question is no, we don't have sufficient understanding of engine damage rates, relative to the dust dose, to be able to back calculate the dust dose from the amount of damage. Evidence of dust damage exists, but we don't know how much dust it takes to get that level of damage. This is why we want accurate – or as accurate as possible – data on the dust in the atmosphere and thus how much dust dose relates to the damage we observe in engines, and hence the motivation for this study.

Further, engine manufacturers *are* beginning to perform controlled laboratory engine dust tests where we know the dose and can relate this to the damage observed However, these are only in their infancy due to extreme costs involved. There are also challenges involved in reproducing in-service dust conditions, and composition of dust adds an additional complexity.

We have added the following text to the introduction to provide more information:

"Mineral dust can cause engine damage through various different mechanisms. A comprehensive description is provided by Clarkson et al. (2020), who describe how dust particles cause erosion of compressor blades, vanes and of seals between engine components, causing loss of efficiency. Dust particles can melt in hot sections of gas turbines (combustors and core turbines) and deposit on surfaces, reducing aerodynamic efficiency, damaging ceramic thermal barrier coatings, and blocking aerofoil film cooling hole features. Dust particles can also enter secondary engine air systems where they restrict cooling air flow, causing overheating or component deterioration. All these processes lead to reduced efficiency and reduced component lifetime. Resultant losses in efficiency can increase aircraft fuel burn and therefore result in increased aviation emissions of greenhouse gases, thus linking mineral dust to aviation's climate impact (e.g. Lee et al., 2021). The damage done by dust depends on the altitude and power of the engine – in part since this determines the quantity of dust ingested, but also because these factors affect dust particles' behaviour during their transit through the engine."

"Reports within the aviation industry suggest that engines operating regularly in dusty airports show evidence of accelerated component deterioration (Clarkson et al. 2020). Although this evidence exists, there is a lack of knowledge of the amount of dust required to cause such damage. Although engine manufacturers are beginning to perform controlled tests where dust concentrations are known and damage is observed, these incur extremely high costs and are currently limited."

Figure 3. I know there are some seasonal and altitude differences, but if you could reorder the entries in the legend for this figure so they are generally in the order of dust concentration magnitude, it would be easier to discern the lines associated with the lowest few, which seem to be Phoenix, Hongkong, and Sydney.

We have rearranged the order of the cities in the legend as suggested.

I understand that you are effectively using seasonal background dust levels for these calculations, and I know that for some phenomena such as dust transport in general, extreme events dominate. So, I'm wondering (a) how well the limited CALIPSO sampling and the CAMS model simulations capture sporadic larger dust events,

(b) whether the airports in question shut down when dust loading is unusually elevated, and (c) how the dosage for even one elevated event for which the airport might remain open might compare with the typical seasonal averages.

These are good questions.

a) For CAMS climatology (e.g. fig 3), where we represent all model events, temporal sampling is not an issue since we use all model output. In terms of how well the model reanalysis represents larger, sporadic events, this is beyond the scope of the study. However, Errera et al. (2021) find that CAMS reproduces the annual variability fairly well compared to AERONET for dust with correlations between 0.84-0.87. They also show that over the Sahara, the largest DOD underestimations are observed during summer, and related to mesoscale convective events which the model cannot reproduce. Errera et al. (2021) and Bennouna et al. (2023) also state that the CAMS reanalysis reproduced a few recent individual large Saharan dust events reasonably well, though AODs are underestimated.

   For CAMS/CALIOP profile and dose comparisons, the temporal sampling potentially becomes important. Figures 4, 5 and supplement figures indicate the number of profiles included in the long-term means shown. For example, taking the Canary Islands for DJF as an example, the CALIOP L3 data includes 146 profiles over 13 years, which is fairly low fraction sampled. Order of magnitude similarities in the sampling also apply to the LIVAS data. Therefore the satellite data are clearly a small sample of the events which occurred. We have not investigated the representativity of CALIOP overpasses as a function of larger dust events. This is beyond the current scope of the work. However, it is reassuring that the CAMS data, also sub-sampled to match the CALIOP overpasses in figure 4/5, shows similar vertical structure and magnitude compared to that using all the data (figure 3), indicating that the climatologies constructed from CALIOP L3/LIVAS sampling are reasonable.

b) Airports and air traffic control have procedures for visibility reductions in place ('Low Visibility Procedures' (LVP) and 'Reduced Aerodrome Visibility Procedures'), which vary depending on how low visibility drops. In extreme events, airports have been reported to have temporarily cancelled or postponed flights due to extreme dust events. When visibility falls beneath around 400m, airports follow these procedures, which generally results in greater spacing between aircraft and therefore reduced airport capacity. We added, "Moderately dusty conditions at airports cause reduced visibility which can require greater spacing between aircraft, and thus reduce airport capacity (ICAO 2023)," to the introduction.

c) Again, this is a very interesting question, but beyond the scope of the current work. Ongoing and future work within our research groups will investigate these questions.

Line 387. The end of the sentence is missing.

Cross-reference to section 5 now included.

Line 576. Might visibility still be an issue in the vicinity of a busy airport, even after an aircraft has left the ground?

No, it isn't a problem. Visibility is a problem on the ground because of the risk of aircraft bumping into other aircraft, ground vehicles and other obstacles. Once the aircraft is in the air the only obstacles to avoid would be other aircraft, but air traffic management procedures keep aircraft a long way apart, whatever the level of visibility. We added, "it is not a concern once aircraft have taken off since air traffic control keep large distances between aircraft, whatever the visibility."

References

Bennouna, Y. et al., 2023, Validation report for the CAMS global reanalyses of aerosol and reactive trace gases: Period 2003-2022, https://atmosphere.copernicus.eu/eqa-reports-global-services

Review 2

The work provides valuable information about the ingestion of atmospheric mineral dust at 10 global airports by using one reanalysis dataset and two observational datasets derived from lidar measurements. The authors compare climatological and seasonal features of dust dose and find substantial differences among the datasets. These differences are discussed in detail. The research design and methodology is considered appropriate. The results are explained in detail and the presentation of the results is adequate, but the discussion of the results could be improved. Please see detailed comments below.

I recommend the article for publication in NHESS after addressing the following comments and recommendations.

We thank the reviewer for this nice summary and positive feedback on our article. Specific comments are addressed below.

Major comment:

The differences between the datasets and therefore dust dose uncertainties are rather large at some airports and I understand that it is important to explain these differences. However, a paper with the title "Aircraft engine dust ingestion at global airports" should not only discuss differences between datasets and data retrievals in the "Discussion" section. I would rather expect some discussion about the results and their implications.

We have added a sentence at the start of the Results section to state that this section presents the main findings, while the discussion goes into more detail of the differences and reasons for these. Since the reasons for the differences between datasets are complex, we consider it clearest to approach them holistically in one section of the article. Additionally, as suggested we have added a new section discussing the implications of the results (more detail below).

My suggestion is the following:

- Move the detailed information about the model and data retrievals to the supplement and condense most important information in the results or the discussion section.

We feel that the details on the model and satellite retrievals are a core part of this study. The most important findings are summarized in the 'summary and conclusions' section. The discussion section is clearly labelled with sub-sections to signpost the reader through that section, as is the model/lidar information in the methods section.

- Compare your results to that of Bojdo et al. (2020) (see comment below) and other studies if available.

We have reduced the description of Bojdo et al. (2020) in the introduction, and added a more detailed comparison of our dose results against theirs in a new section in the Discussion, "Comparison with Existing dust dose estimations."

- Discuss the model results in terms of magnitude: Since CAMS < CALIOP < AERONET < MODIS, CAMS might significantly underestimate dust concentration at several locations. What does that mean for aircraft engines?

We have added a new section to the discussion, 'Implications of Dataset Differences' where we discuss this, particularly the CAMS < both CALIOP datasets point, since CAMS is beginning to be widely used in the aviation sector. We also added an implication statement to the abstract regarding this point.

- Discuss the implications of a jet engine core ingesting dust (text from conclusion section, lines 594 to 610). Could you give more detailed information about the specific types of damage? Is there any critical mass of dust? Please give more information, if possible.

More information has been added to the introduction to provide more detail on the specific types of damage incurred by engines due to dust (see track changes in the manuscript and response to reviewer 1).

- Regarding the concept of a critical mass, or more accurately a critical dose, all the damage mechanisms now described in the introduction have a long-term impact; they don't cause rapid failures during or shortly after the dust exposure, unlike some of the high profile volcanic ash exposures. And although volcanic ash – with its high glass content – is more likely to cause very rapid build-up of deposits in the hot section, leading to compressor stall and engine shutdown, mineral dust can do this too, at high enough concentrations. But the concentrations needed are in the 100 mg/m3 range rather than 0.1-10 mg/m3 associated with very dusty conditions.
- The actual mass of deposit in a turbine section needed to get a volcanic ash type failure does vary depending on specific engine type, but is about 0.5 – 1 kg, noting that to get this in the turbine the engine core needs to ingest about 10 times this, i.e. a core dose of around 5 – 10 kg – or about 1000 flights out of somewhere like Doha. And just for good measure, the concentration of the dust going into the engine would still have to be at around 50-100 mg/m3; at lower concentrations most of the deposit will have been shed before sufficient can build up. It's a complex topic that would require a separate paper.

Minor comments:

Lines 21/22: You explicitly mention Beijing's dust dose in the abstract. Why? I suggest either removing the sentence or explaining why this information is important.

This sentence has been changed to, "Dust doses are mostly largest in northern hemisphere summer for descent, with the largest at Delhi in JJA (6.6 g) followed by Niamey in MAM (4.7 g) and Dubai in JJA (4.3 g)."

Lines 65 to 72: While the work of Bojdo et al. (2020) should definitely be mentioned in the introduction, I recommend moving the description of their work including the discussion of their findings to your discussion section (see major comment above).

See response to major point above. We have added a more substantial comparison to Bojdo et al. (2020) and moved some sections of text around.

Line 101: Did the authors also investigate dust dose at the airport in Singapore? If not, please rewrite this sentence.

Corrected

Line 124, Line 661: Please consistently write "analyse" or "analyze".

Done

Line 147: Please consistently use data as singular or plural noun (plural noun: e.g., lines 116, 153, 287, 357, 657, 680; singular noun: e.g., lines 147, 187, 541, 570).

Changed to singular.

Line 157: The "Young et al. 2018" reference is missing in the reference list.

Added

Lines 183/184: I do not understand this sentence. Please clarify.

'is generated' added to the sentence.

Lines 187 to 189: Did you do this in your study or is this part of the LIVAS processing? Please clarify and add a remark.

The re-gridding was done for our study – this sentence has been reworded to clarify.

Line 203: “two products are not similar”: what does “not similar” mean? How big are these differences? This sentence seems to be the condensed version of Section 5.2 (see major comment above).

We removed this sentence as it was not necessary. This section only describes the methodological differences between LIVAS and CALIOP L3. Section 5.2 is intended to discuss the impacts of the differences on the results.

Lines 219/220: “We choose to compare the profiles using mass, since this is the metric of interest to the aviation community, though we note that extinction comparisons showed the same results.”: The authors could show these results in the supplement.

Since the results show the same proportional differences and vertical structures, we do not consider it necessary to include them in the supplement.

Line 223: “Dust dose is defined as the total mass (g) of dust”: When using equation 2, the unit of total mass is “kg” rather than “g”.

Changed to kg

Line 241: What does “lbf” mean?

Changed to ‘pounds-force’

Figure 2: Please use the same y-axis for both panels. Figure caption: add “(blue)” after “altitude” and “(black solid line)” after “wcore”.

Changed

Lines 265 to 267: “All airports show the highest mean dust concentrations in JJA (driven by peak solar heating and dry convection over northern hemisphere desert regions) except Beijing and Niamey.”: What about Sydney, which is located in the southern hemisphere?

We moved the sentence, “Sydney, Phoenix, Hong Kong and Bangkok all display mean dust concentrations below 10 µgm-3., and are not discussed further,” to the start of this paragraph to clarify that these lines do not describe these cities.

Line 272: “Sydney, Phoenix, Hong Kong and Bangkok all display mean dust concentrations below 10 µg m-3.”: The authors should add here that these airports will not be discussed later on.

See above point.

Figure 4: Is the different number of CALIOP L3 and LIVAS overpasses related to the different dust products (pure-dust vs. dust also from polluted dust products)?

Yes, this is correct. CALIOP L3 data do not include polluted dust categories (see section 2.3.1). However, LIVAS data apply the CALIOP L2 'pure dust,' 'polluted dust' and 'dusty marine' categories, extracting the 'pure dust' component from them (see section 2.3.2). Therefore the number of profiles contributing to each dataset is different, with LIVAS including more profiles. Some of the consequences of this are discussed in the Discussion.

Lines 359 to 383: Compared to the description and discussion of the other figures, this text gives to much detailed information and some aspects are not clear. For example: lines 359/360: "…CALIOP L3 substantially larger than both, are most evident at airports with a low altitude dust plume, particularly Niamey in DJF/MAM and Dubai year-round." In Niamey, the DJF and MAM medians of both LIDAR datasets are in very good agreement. In Dubai, the DJF and SON medians of both LIDAR datasets are also in very good agreement. Please clarify and shorten the text.

The text has been adjusted slightly to clarify, "The largest differences, with LIVAS and CALIOP L3 values larger than CAMS, and CALIOP L3 frequently larger than LIVAS, are most evident at airports with a low altitude dust plume, particularly Niamey in DJF/MAM and Dubai year-round." And later on, "Differences between CALIOP L3 and LIVAS in these cases are most marked when the hold altitude mass concentrations differ." We believe that this figure presents the core results of our study, and that therefore the description length is justified.

Lines 389/390: "For departure (see supplement), overall the similarities and differences between the datasets are the same as for arrival, with lower doses for departure by 10 to 23%.": Do these numbers refer to the median or to the lower/upper quartile?

This refers to the median (clarified in text).

Lines 390/391: "However, in a few cases differences between datasets compared to arrival are sensitive to the overall vertical profile shape and magnitude, particularly if ground concentrations are very large." Isn't this always the case because of the location of the hold altitude?

No – here we aim to explain that generally descent dose is larger due to the hold pattern contribution to dose. However, in a few cases this is the opposite: ascent dose is larger than descent. We reworded this section to read:

"For departure (see supplement), overall the similarities and differences between the datasets are the same as for arrival, with lower median doses for departure by 10 to 23%, due to the lack of hold phase dose contribution during ascent. However, in a few cases doses are higher for departure than arrival. This is because differences between datasets are sensitive to the overall vertical profile shape and magnitude, particularly if ground concentrations are very large."

Lines 401 to 403: "This is partly a feature of the larger magnitudes seen in the lidar data compared to CAMS, but also due to the lower sampling rate for CALIPSO compared to the regular 3 hourly model output from CAMS.": Did you use all CAMS data or only CAMS data coincident with CALIOP measurements? Please clarify.

We only use CAMS data which was coincident with CALIOP L3 sampling times in Section 3.2.2 onwards (i.e. comparisons between CAMS/lidar). This has been added to section 2.2. ("When compared against spaceborne lidar data, CAMS data are restricted to overpass times for comparison purposes.") The sentence referred to by the reviewer has been deleted as it was potentially misleading, now reading, "This is partly a feature of the larger magnitudes seen in the lidar data compared to CAMS, but and perhaps an indication that CAMS does not represent infrequent, larger dust events particularly well."

Lines 437/438: "For the peak dust seasons, a reduction in dose of 41% at Dubai in JJA, 34% at Delhi in JJA and 39% at Niamey in DJF could be achieved.": I try to understand how you calculated these numbers by looking at Delhi: According to Figs. 6 and 7, maximum dust dose in JJA is 6.6 g and 4.4 g for arrival and departure, respectively. This sums up to 11 g. However, according to Table 1, the reduction of 34 % refers to 6.44 g, which indicates that total dust was approximately 19 g. Where does this difference come from? Please clarify.

The values in Table 1 refer to reductions (g) and percentage differences between dose at the *maximum* and *minimum* during the diurnal cycle, rather than the diurnal mean as shown in figures 6 and 7. Values in Table 1 are calculated from seasonal airport mean doses, separated into 3 hourly intervals, incorporating both an ascent and a descent. E.g. for Delhi in JJA, once we have doses for every 3 hours of the day, as a climatological mean, we subtract the time of day with the lowest dose from the time of day with the highest dose. This gives the reduction in dose and its percentage equivalent (here ~6.4 g reduction from a maximum of ~19g). The manuscript states, "we show the reduction in dust dose possible for each the six dustiest airports between the maximum and minimum throughout the diurnal cycle, for an arrival immediately followed by a departure, equivalent to aircraft delaying arrival and departure from late afternoon to night time."

We adjusted the caption of table 1 slightly to read, "Seasonal mean reduction in dust dose between maximum and minimum throughout the diurnal cycle for an arrival directly followed by a departure for the CAMS dataset, given in g and as a percentage."

Table 1: Please specify only one decimal place for dose reduction.

Done

Lines 484/485: "without mixing from other aerosol types (e.g., Marrakesh and the Canary Islands)": What about sea salt aerosols in Canary Islands? Please clarify.

During the peak dust season at the Canary Islands (boreal summer) the dust plume is elevated (i.e. not at the same altitude as marine aerosol) and most of the aerosol mass and optical contribution comes from dust, rather than other aerosol types.

Section 6: Conclusion: I'd suggest renaming this section to "Summary and conclusions".

Done

Lines 633/634: “resulting in a mean underestimate by CAMS of 2.4 over both datasets”: I do not understand the relevance of the mean bias over both lidar datasets. I suggest removing this part of the sentence.

Agreed, this has been removed and the figures in the abstract adjusted to reflect this change.

Lines 657 to 660: I suggest moving these two sentences to line 650 and mentioning that the results discussed before were based on the CAMS reanalysis.

We feel that these sentences fit in here as they correspond to limitations/further work relating to the diurnal dust dose findings. We have added a few extra words to signpost the reader better through this paragraph in the manuscript.

Supplement, Figure S5: Canary Island and Delhi: LIVAS data are missing.

These have been included.

Editorial:

Line 21: add “northern hemisphere” before summer.

Done

Line 25: Add “instrument” after (CALIOP).

Should not be required since the sentence indicates it’s a lidar.

Line 29: “up to 44% and 41% respectively” rather than “up to 44% or 41% respectively”, I think.

Changed

Section 1: remove “1”.

Changed

Line 49: “O’Connell” rather than “O’connell”.

Changed

Line 64: “(Inness et al. 2019)” rather than “(Inness et al. (2019))”.

We believe the text is correct, due to the use of 'e.g.' in the sentence. We leave this decision to ACP copy-editing.

Line 76: "CAMS forecasts and reanalyses" rather than "CAMS forecasts and reanalysis".

The CAMS reanalysis is singular.

Line 81: Add a reference after "dust properties", e.g., Mona et al. 2012, doi:10.1155/2012/356265.

We added Winker et al. (2007).

Line 83: Add "instrument" after "(CALIPO)".

The sentence indicates it is a lidar, so we do not consider this addition necessary.

Line 84: "(e.g. Liu et al. 2008a; Yang et al. 2013; Song et al. 2021)" rather than "(e.g. Liu et al. (2008a); Yang et al. (2013); Song et al. (2021))".

We believe the text is correct, due to the use of 'e.g.' in the sentence. We leave this decision to ACP copy-editing.

Line 86: "12-year period" rather than "12 year period".

Line 93: "Section 5 concludes": This is not true. Section 5 is the "Discussion" section, Section 6 concludes.

Changed

Line 99: Please exchange "Bejing" and "Bangkok" to follow the numbering.

Done

Line 100: "'dust belt'," rather than "'dust belt,'".

Commas should be placed inside speech marks.

Line 103/104: add "coarse" before "model resolution" and refer to Section 2.2.

Done

Line 113: Introduce "ECMWF".

Done

Line 121: “lower/upper diameters” rather than “upper/lower diameters”.

Done

Line 141/142: I suggest moving the sentence “The CALIPSO orbit track….” to line 134 (after the Winkler et al. (2010) reference.

Done

Line 142: Add a break before “Here we analyze…”.

Done

Line 158: “reported by Floutsi et al. (2022)” rather than “reported by (Floutsi et al., 2022)”.

Changed

Line 160: add “latitude-longitude” before “grid”.

Done

Line 161: Add a break before “We use the extinction coefficient”.

Done

Line 161: “extinction coefficient profiles at 532 nm” rather than “extinction coefficient at 532 nm profiles”.

Done

Lines 165, 207: “CALIOP” rather than “CALIPSO”.

Done

Line 166: “an altitude of 90 m” rather than “an altitude 90 m”.

We feel the wording is acceptable here.

Line 172: (LIVAS, Amiridis et al., 2015) rather than “(LIVAS, Amiridis et al. (2015))”.

This is an in-sentence citation due to the word LIVAS and cited as author (year).

Line 174: “EARLINET, Pappalardo et al., 2014; last” rather than “EARLINET, Pappalardo et al. (2014); last”.

Done

Lines 180 and 197: "'pure dust', 'dusty marine'," rather than "'pure dust,' 'dusty marine,'".

Commas should be placed inside inverted commas.

Line 191: add "as input" after "profiles".

Done

Line 202: "sr" rather than "Sr".

Done

Lines 202/203: "(Amiridis et al., 2013; Marinou et al., 2017; Proestakis et al., 2018; Floutsi et al., 2022, see supplement)" rather than "((Amiridis et al., 2013; Marinou et al., 2017; Proestakis et al., 2018; Floutsi et al., 2022), see supplement)".

We leave this decision for copy-editing.

Line 224: "from Clarkson (2020)" rather than "from (Clarkson, 2020)".

Done

Line 226: add "(dimensionless)" after "regime".

Done

Line 235: "thermodynamics" rather than "theromodynamics".

Done

Line 252: "discuss" rather than "test".

We leave this as 'test' since we do indeed test the sensitivity.

Line 301: "are" rather than "were", I think.

Done

Line 304: "show" rather than "showed", I think.

Done

Line 313: “greater than 2 g in winter”: it is even greater than 3 g in winter.

That is correct, but not the point we are making.

Line 316: “contributes to at least 50%” rather than “contributes at least 50%”, I think.

Done

Line 350: remove “to those calculated from”.

Sentence adjusted.

Figure 8: Please use the same y-axis for all panels; please capitalize the first letter of each airport name. Does it make sense to use an exponential y-axis?

These changes have been made. We changed the y-axis to a semi-log axis to make better use of the figure space.

Line 387: The Section number is missing.

Done

Line 433: “for the six dustiest airports” rather than “for each airport”.

Done

Line 438: “an” rather than “a an”.

Done

Line 439: Maximum reduction is 19 % in Canary Islands.

Changed

Line 482: remove “the reason” after “explain”.

Done

Line 489: “(e.g., Zhao et al., 2022)” rather than “(e.g., Zhao et al. (2022))”.

We believe the text is correct, due to the use of 'e.g.' in the sentence. We leave this decision to ACP copy-editing.

Lines 495/496: "(e.g., Schuster et al., 2012; Sayer et al., 2018; Song et al., 2021)" rather than "(e.g. Sayer et al. (2018); Schuster et al. (2012); Song et al. (2021)".

We believe the text is correct, due to the use of 'e.g.' in the sentence. We leave this decision to ACP copy-editing.

Line 500: "DOD" rather than "DAOD".

Changed

Line 509: "O'Sullivan" rather than "O'sullivan".

Changed

Line 526: "sr" rather than "Sr".

Done

Line 578: Add a break before "This study…".

Done

Line 599: "representative of the region around" rather than "representative of region around".

Done

Line 613: "spent there, which" rather than "spent in the hold pattern, which".

We feel this wording makes the meaning of the sentence clear.

Line 625: "the vertical structure at Beijing" rather than "the vertical structure shape at Beijing".

Done

Line 642; remove "both" before "dust properties".

Done

Line 652: add "by increasing hold altitude from 1 km to 3 km" after "can be reduced by 41%".

This figure does not refer to hold altitude change, therefore we leave the sentence unchanged.

425

Aircraft Engine Dust Ingestion at Global Airports

Claire L. Ryder[1], Cléèment Bézier[1,2], Helen F. Dacre[1], Rory Clarkson[3], Vassilis Amiridis[4], Eleni Marinou[4], Emmanouil Proestakis[4], Zak Kipling[5], Angela Benedetti[5], Mark Parrington[6], Samuel Rémy[7], Mark Vaughan[8]

[1]Department of Meteorology, University of Reading, Earley Gate, PO Box 243, Reading, RG6 6BB, UK
[2]Service des Avions Français instrumentés pour la Recherche en Environnement (SAFIRE), Météo-France, CNRS, CNES, Toulouse, France
3 Rolls-Royce plc, Derby, UK
4 National Observatory of Athens, IAASARS, Athens, 15236, Greece
5 ECMWF, Shinfield Park, Reading, RG2 9AX, UK
6 ECMWF, Robert-Schuman-Platz 3, 53175 Bonn, Germany
7 Hygeos, Lille, France
8 NASA Langley Research Center, Hampton, VA, USA

Correspondence to: Claire Ryder (c.l.ryder@reading.ac.uk)

Abstract. Atmospheric mineral dust aerosol constitutes a threat to aircraft engines from deterioration of internal components. Here we fulfil an outstanding need to quantify engine dust ingestion at worldwide airports. The vertical distribution of dust is of key importance since ascent/descent rates and engine power both vary with altitude and affect dust ingestion. We use representative jet engine power profile information combined with vertically and seasonally varying dust concentrations to calculate the 'dust dose' ingested by an engine over a single ascent or descent. Using the Copernicus Atmosphere Monitoring Service (CAMS) model reanalysis, we calculate climatological and seasonal dust dose at 10 airports for 2003-2019. Dust doses are mostly largest in northern hemisphere summer for descent, with the largest at Delhi in JJA (7.5~~6.6~~ g) followed by Niamey in MAM (4.0 g) and Dubai in JJA (4.5 g). ~~Beijing's largest dose occurs in spring (2.9 g)~~. Holding patterns at altitudes coincident with peak dust concentrations can lead to substantial quantities of dust ingestion, resulting in a larger dose than the take-off, climb and taxi phases. We compare dust dose calculated from CAMS to spaceborne lidar observations from two dust datasets derived from the Cloud–Aerosol Lidar with Orthogonal Polarization (CALIOP). In general, seasonal and spatial patterns are similar between CAMS and CALIOP though large variations in dose magnitude are found, with CAMS producing lower doses by a ~~mean~~ factor of 1.9 to 2.8~~2.4±0.5~~, particularly when peak dust concentration is very close to the surface. We show that mitigating action to reduce engine dust damage could be achieved, firstly by moving arrivals and departures to after sunset and secondly by altering the altitude of the holding pattern away from that of the local dust peak altitude, reducing dust dose by up to 44% ~~or~~ and 41% respectively. We suggest that a likely low bias of dust concentration in the CAMS reanalysis should be considered by aviation stakeholders when estimating dust-induced engine wear.

1 ~~1~~ Introduction

Aircraft gas turbine engines ingest ambient atmospheric gases and aerosols in addition to pure air. Many atmospheric components cause damage to internal components of aircraft engines, through erosion, corrosion or deposition (Clarkson, 2019). Since the volcanic eruption of Eyjafjallajökull in 2010, which closed down most European airspace for over 5 days and caused $5 billion in economic losses (Prata and Rose, 2015; Prata et al., 2018), renewed focus has been given to the impact of volcanic ash on aircraft engines. High concentrations of volcanic ash can compromise safety and thus the highest ash concentrations must be avoided (Clarkson et al., 2016). Mineral dust, originating from arid regions and uplifted by strong surface winds (Knippertz and Stuut, 2014), also causes damage to aircraft engines (Clarkson, 2019). It is generally unlikely to be a safety issue in itself, instead causing engine components to degrade more rapidly, impacting efficiency and maintenance costs. Indirectly, icing caused by mineral dust particles acting as ice nuclei can be a serious threat to aviation (Nickovic et al., 2021). Despite this, under extremely dusty conditions, operations are more likely to be cancelled due to visibility reductions rather than risk to aircraft engines (Middleton, 2017). Moderately dusty conditions at airports cause reduced visibility which can require greater spacing between aircraft, and thus reduce airport capacity (Icao, 2023).

Mineral dust can cause engine damage through various different mechanisms. A comprehensive description is provided by Clarkson et al. (2020), who describe how dust particles cause erosion of compressor blades, vanes and of seals between engine components, causing loss of efficiency. Dust particles can melt in hot sections of gas turbines (combustors and core turbines) and deposit on surfaces, reducing aerodynamic efficiency, damaging ceramic thermal barrier coatings, and blocking aerofoil film cooling hole features. Dust particles can also enter secondary engine air systems where they restrict cooling air flow, causing overheating or component deterioration. All these processes lead to reduced efficiency and reduced component lifetime. Resultant losses in efficiency can increase aircraft fuel burn and therefore result in increased aviation emissions of greenhouse gases, thus linking mineral dust to aviation's climate impact (e.g. Lee et al. (2021)). The damage done by dust depends on the altitude and power of the engine – in part since this determines the quantity of dust ingested, but also because these factors affect dust particles' behaviour during their transit through the engine.

Reports within the aviation industry suggest that engines operating regularly in dusty airports show evidence of accelerated component deterioration (Clarkson et al. 2020). Although this evidence exists, there is a lack of knowledge of the amount of dust required to cause such damage. Although engine manufacturers are beginning to perform controlled tests where dust concentrations are known and damage is observed, these incur extremely high costs and are currently limited.

In recent years the potential for dust-related engine damage has increased as a result of increased flight operations in dusty regions and greater susceptibility of engine parts to dust damage. This is firstly, due to a move towards more fuel-efficient engines which employ hotter, higher pressure cores with tighter clearances, more complex cooling systems and more

sophisticated protective coatings, resulting in engines which are less tolerant to dust as well as other atmospheric contaminants (Clarkson, 2019). Secondly, air traffic activity has significantly increased in arid, dusty areas (particularly the Middle East), increasing aircraft exposure to mineral dust (O'connell and Bueno, 2018). Increased air traffic worldwide means that infrequent but large dust events are also more likely to impact air traffic. Thirdly, there has been a shift away from airlines directly funding engine repair and overhaul – under time and material arrangements with overhaul bases – to service contracts where they pay an overhaul provider (usually the engine manufacturer) a fee per flight hour, transferring the repair and maintenance liabilities to that overhaul provider. Combined with increased economic pressure on airlines to maximise operations, this has resulted in increased likelihood for aircraft to operate in dusty conditions, especially as dust does generally not represent an aviation safety threat.

The amount of dust ingested by aircraft engines depends on both the total dust concentration, its vertical distribution, and spatial and temporal variations as well as the engine power which varies with time and altitude. There is an outstanding need to quantify aircraft dust dose (the total dust mass ingested over a given amount of time), particularly due to the vertical distribution of dust, since this varies spatially, seasonally, and diurnally depending on location and dominant meteorology in uplifting and transporting dust plumes. Since different aircraft will ingest differing amounts of air (and therefore dust) during different phases of aircraft ascent and descent as a result of varying engine power and duration (Clarkson, 2020), the vertical distribution of dust will have a key influence on engine dust ingestion.

Model reanalyses of atmospheric composition, which include mineral dust aerosol (e.g., Inness et al. (2019)), are a powerful tool in quantifying dust concentrations and their variability in space and time. Bojdo et al. (2020) used ECMWF hindcasts from the Copernicus Atmosphere Monitoring Service (CAMS) to calculate engine dust dose at Doha airport for an Airbus A380-841 with Rolls-Royce Trent 900 engines. ~~They found that the average dust dose ingested into the engine core per flight was 8.5 g, with peak dust ingestion occurring just after take-off and during aircraft transition into climb phase at around 1 km. Additionally, they found that a twenty minute hold phase over the dusty Persian Gulf at around 3 km accumulated a dose of 8 g.~~ They focused their study on three dusty months ~~at Doha at 6 h temporal resolution~~specifically. However, an assessment of engine dust dose at a wider range of airports, over a larger temporal range, and a higher sampling rate of diurnal variability has not yet been undertaken.

Accounting for the vertical distribution of dust is vital in calculating dust dose and for models of particle damage to engine components (Ellis et al., 2021; Bojdo et al., 2020). Spatial distributions and vertically resolved dust concentrations are available from atmospheric models incorporating mineral dust schemes, such as the CAMS forecasts and reanalysis. Although CAMS has the advantage of assimilating total aerosol optical depth retrieved from satellite observations, there are no constraints on how this is proportioned across different aerosol types or in the vertical dimension. Many satellite sensors measure aerosol optical depth, but there are challenges in proportioning this into dust-specific components and little-to-no

information on the vertical distribution. One exception to this is spaceborne and ground-based lidars, which provide vertically resolved profiles of dust properties (e.g. Winker et al. (2007)). The importance of height-resolved dust information from ground-based lidars has been highlighted for near real-time aviation warnings (Papagiannopoulos et al., 2020). Lidar observations from the spaceborne Cloud–Aerosol Lidar with Orthogonal Polarization (CALIOP) have proved invaluable in characterizing the vertical distribution of dust and its regional variations (e.g. Liu et al. (2008a); Yang et al. (2013); Song et al. (2021)).

Here we use time-varying three-dimensional dust concentration from the CAMS reanalysis over a 12 year period to determine climatological engine dust dose for a range of worldwide airports, for a single ascent or descent manoeuvre (i.e., departure or arrival). We investigate the dust vertical profiles in different regions which occur due to varying regional meteorology and how these affect dust dose, as well as the contribution from seasonal and diurnal variability in vertical profiles. Finally, we compare the reanalysis dust profiles and associated dust dose to observational spaceborne lidar retrievals of vertically resolved dust concentration from two CALIOP dust datasets. Section 2 describes the method, datasets and dose calculations, Section 3 presents results of vertical profile dust climatologies and dose climatologies, Section 4 provides potential dose mitigation methods, Section 5 discusses the findings, Section 6 concludes.

2 Methods

2.1 Selection of airports

This work focuses on a selection of ten airports, selected based on air traffic activity levels, proximity to dusty regions and anecdotal reports of dust ingestion. The airports selected are Phoenix, the Canary Islands, Marrakesh, Niamey, Dubai, Delhi, Beijing, ~~Bangkok~~, Hong Kong, Bangkok ~~Beijing~~ and Sydney, as shown in Figure 1. Broadly, The African and Asian airports are located in or around the edges of the well-known ‘dust belt,’ stretching from western Africa through to Northern China (Prospero et al., 2002). ~~Singapore,~~ Hong Kong and Bangkok are located south of major dust transport pathways but serve as major airports in the region and aircraft have reported occasional dust damage here. Sydney and Phoenix can be affected by large but infrequent dust storms originating from arid areas in eastern Australia and the western US (Ginoux et al., 2012). Due to the coarse model resolution (see Section 2.2), the Canary Islands covers all airports on the islands.

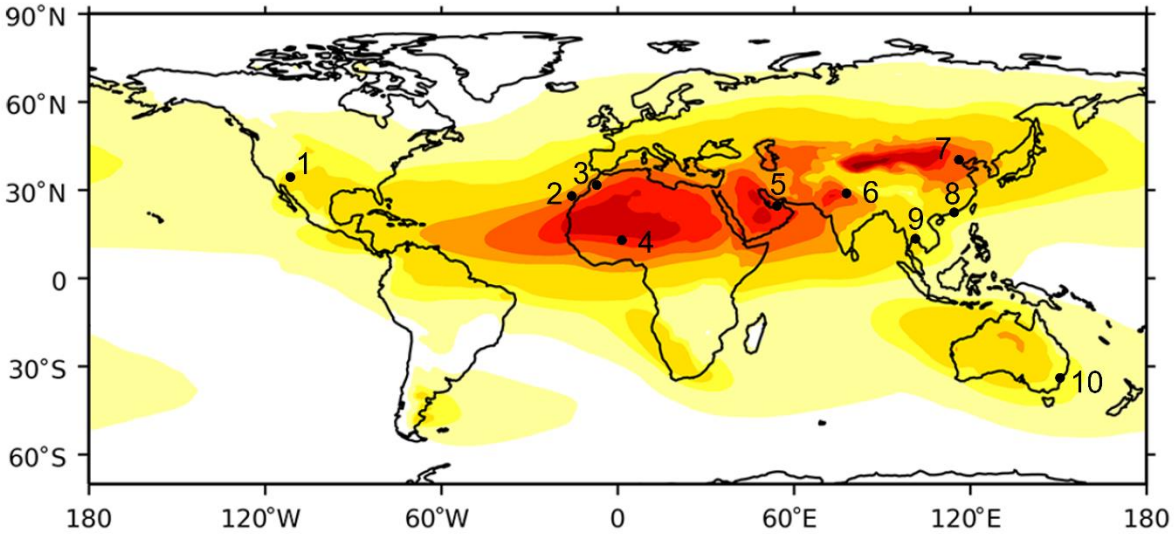

Figure 1: Airport locations used in this study. 1= Phoenix, 2=Canary Islands, 3=Marrakesh, 4=Niamey, 5=Dubai, 6=Delhi, 7=Beijing, 8=Hong Kong, 9=Bangkok, 10=Sydney. Underlying contours show distribution of annual average column dust loading from CAMS from 2005-2014, adapted from Zhao et al. (2022).

2.2 CAMS Reanalysis Dust Concentrations

We utilize the global Copernicus Atmosphere Monitoring Service (CAMS) reanalysis dataset (Inness et al., 2019) to estimate climatological, vertically resolved dust mass concentrations at each airport. Aerosol and meteorological modelling and data assimilation are carried out by the European Centre for Medium Range Weather Forecasting (ECMWF) Integrated Forecast System within the CAMS framework. Total aerosol optical depth (AOD, covering all aerosol species) from satellite retrievals are assimilated into CAMS, and concentrations of individual aerosol species are adjusted according to the modelled proportions and vertical distributions of each aerosol type, of which mineral dust constitutes one of five (Morcrette et al., 2009). CALIOP data are not included in the assimilation. Thus, the CAMS dataset benefits from an observational constraint of AOD, affecting total aerosol column load, though how this is proportioned amongst different aerosol types and their vertical distribution is dependent on the model-simulated values. Dust emission is driven by modelled surface wind speed, soil moisture, surface albedo and bare soil fraction conditions (Bozzo et al., 2020; Morcrette et al., 2008; Rémy et al., 2019). Dust is represented by three size bins with ~~upper/~~lower/upper diameters of 0.06, 1.1, 1.8 and 40 µm, and transport following emission is controlled by model winds and associated meteorology.

We analyse data from January 2003 to December 2019, though in comparisons to spaceborne lidar we restrict this to 2007-2019 to be consistent with that data. The nearest CAMS grid box (size of 80 km) to the location of each airport is selected. Dust mass mixing ratios are available at 3 hourly time intervals with 60 vertical levels of which we use 23, corresponding to the surface to approximately 6 km altitude. Total dust concentrations are calculated as the sum of dust over the 3 size bins,

and by converting mass mixing ratios (kg/kg) to dust mass concentration (kg/m^3) as a function of altitude using standard meteorological conversions. Climatologies are calculated as monthly mean profiles for each airport using 3 hourly output data from CAMS. When compared against spaceborne lidar data, CAMS data are restricted to overpass times for comparison purposes.

2.3 CALIOP Spaceborne Lidar

As an observational comparison to the CAMS dust profiles, we use spaceborne lidar data from the Cloud–Aerosol Lidar with Orthogonal Polarization (CALIOP) instrument aboard the Cloud–Aerosol Lidar and Infrared Pathfinder Satellite Observations (CALIPSO) satellite (Winker et al., 2010). The CALIPSO orbit track repeats every 16 days, (until 2018 when the orbit was adjusted), though global coverage is never achieved due to the small footprint size. CALIOP is an elastic backscatter lidar, providing information on the spatial and vertical distribution of aerosols at wavelengths of 532 nm and 1064 nm. Attenuated backscatter profiles are measured, from which aerosol extinction profiles are derived, where extinction is the absorption and scattering coefficient at each height, broadly indicating the amount of aerosol in the atmosphere. Additionally, CALIPSO measures the linear depolarization ratio at 532 nm, enabling identification of dust aerosols, which are strongly depolarizing due to their non-spherical shape, in contrast to other aerosol types (Kim et al., 2018). CALIOP therefore provides an observationally driven estimate of the vertical distribution of dust, although limitations exist and certain assumptions are required, as described below. ~~The CALIPSO orbit track repeats every 16 days, (until 2018 when the orbit was adjusted), though global coverage is never achieved due to the small footprint size.~~

Here we ~~analyze~~analyse two different 532 nm CALIOP datasets: the standard Level 3 dataset, produced and distributed by NASA's CALIPSO project, (henceforth referred to as 'CALIOP L3') and the LIdar climatology of Vertical Aerosol Structure (LIVAS) dataset, created from the CALIPSO measurements (Amiridis et al., 2015; Amiridis et al., 2013). For purposes of comparison to CAMS, the CALIOP datasets are both reduced to the same vertical resolution of CAMS. For both datasets we use night time data only in order to retrieve maximum lidar signal-to-noise ratios in the absence of solar radiation. For comparisons between the lidar datasets and CAMS, CAMS data ~~is~~ are also restricted to night hours and dates of the coincident overpass for consistency. We now describe the different processing between the CALIOP L3 and LIVAS datasets.

2.3.1 CALIOP L3

We use the Level 3 (L3) version 4.20 monthly mean 'Tropospheric Aerosol Cloud Free' product provided by NASA (Tackett et al., 2018), which currently provides the longest observational record of the vertical distribution of speciated aerosol. L3 data are derived from the Level 2 (L2) V4.20 data product where 532 nm integrated attenuated backscatter, estimated particulate depolarization, altitude, location, and surface type are used to identify the dominant aerosol type in a layer. In particular, if the layer-integrated depolarization ratio exceeds 0.20 (indicating non-spherical particles), then the

layer is identified as 'dust.' A fixed lidar ratio of 44 sr is used to convert the measured dust attenuated backscatter coefficient profiles to extinction coefficient profiles ~~(Kim et al., 2018,~~ (Young et al., 2018; Kim et al., 2018)~~Young et al., 2018)~~. This lidar ratio value is in agreement with the averaged ground-based lidar ratio measurements for desert dust, recently reported by Floutsi et al. (2022), despite the regional dependence. L2 data are averaged and quality controlled to produce the L3 product, which provides monthly mean extinction profiles as a function of aerosol type (Tackett et al., 2018). CALIOP L3 data are produced on a 2°× 5° latitude-longitude grid with a vertical resolution of 60m, up to 12 km altitude.

We use the 532 nm extinction coefficient ~~at 532 nm~~ profiles of atmospheric features classified as 'dust' aerosol. We use cloud-free conditions for night time ~~CALIPSO~~ CALIOP overpasses only, in order to minimize uncertainties from cases contaminated by clouds overlying dust layers and by high sunlight illumination conditions (low signal to noise ratio). We exclude the 'polluted dust' and 'dusty marine' aerosol types. In very dusty cases, in-layer attenuation may mean that the ~~CALIPSO~~ CALIOP feature detection algorithm does not detect the entire vertical extent of a dust layer, and the layer base will be assigned an altitude 90 m above Earth's surface. Data beneath this altitude (or layer) do not contribute to the summed extinction coefficient profile or sample count of atmospheric layers classified as 'dust' in terms of aerosol-subtype (Tackett et al., 2018). Each CALIOP L3 airport gridbox is selected to encompass the equivalent CAMS gridbox. Although the CALIOP gridbox is larger than that from CAMS, the results showed negligible sensitivity to including multiple CAMS gridboxes for the comparison. We use data covering 2007 to 2019.

2.3.2 LIVAS

We use the 'pure dust product' from the LIdar climatology of Vertical Aerosol Structure (LIVAS, Amiridis et al. (2015)). The LIVAS pure-dust dataset (Amiridis et al., 2013) is established based on CALIOP L2 V4.2 aerosol and cloud profiles and findings from the European Aerosol Research Lidar Network (EARLINET, Pappalardo et al. (2014)~~,~~; last access: 23/08/2022). LIVAS was developed to provide pure-dust and non-dust components of atmospheric scenes under the assumption of external aerosol mixtures (Tesche et al., 2009). The LIVAS 'pure-dust' product applies CALIOP L3 quality assurance parameters to height-resolved particulate depolarization ratio and backscatter coefficient profiles at 532 nm (Konsta et al., 2018) to decouple the contributions from non-spherical (dust) aerosol and other (non-dust) spherical aerosol components of the backscatter profile (Amiridis et al., 2013; Kim et al., 2018). LIVAS analyses are limited to those CALIOP L2 profiles already classified by CALIOP as either 'pure dust,' 'dusty marine,' or 'polluted dust' (Kim et al., 2018). If the particulate linear depolarization retrieved by CALIOP in any vertical bin is greater than 0.31 for pure dust (Floutsi et al., 2022), the whole volume in that vertical bin is considered dusty; if it lies between 0.05 to 0.31 then the aerosol is assumed to consist of mixed species and the proportion of backscatter derived from dust aerosol is calculated. Through the sum of these signals, the profile of 'pure-dust' backscatter coefficient at 532 nm is generated. A region-specific lidar ratio (see supplement for values) is then used to calculate 'pure-dust' extinction coefficient profiles from the backscatter coefficient profiles (Amiridis et al., 2015; Marinou et al., 2017; Proestakis et al., 2018; Floutsi et al., 2022). Here we use the LIVAS 'pure dust

extinction coefficient product' for cloud-free, night-time cases. We convert the LIVAS data to~~, on~~ a~~n~~ ~~identical~~ 2°×5° grid ~~to match the CALIOP L3 data~~, for the years 2007 to 2019 in order to match the CALIOP L3 data. In cases where data ~~is~~ are affected by a strong return signal from the ground in the lowest two altitude bins, a value from the first altitude above 100m is replicated downwards.

2.3.3 Differences between CALIOP L3 and LIVAS

In summary, both CALIOP L3 and LIVAS use CALIOP L2 V4.2 profiles as input. Both approaches use a particulate depolarization threshold to identify dust profiles, though in each dataset this is applied in very different ways. The CALIOP L2 analyses retrieve aggregate extinction coefficients from detected aerosol layers based on a single aerosol subtype classification (one of which is 'dust') applied to the entire layer. For heterogeneous layer types (e.g., dusty marine and/or polluted dust), CALIOP L3 does not attempt to partition the total extinction into disjoint dust and 'not dust' components. ~~As a result~~Therefore~~,~~ the CALIOP L3 data used here includes only the 'pure dust' aerosol layer type. In contrast, LIVAS separately extracts the 'pure dust' extinction component from all CALIOP dust aerosol types, including the 'dust,' 'dusty marine,' and 'polluted dust' categories. Consequently, LIVAS can fully describe the spatial and temporal distributions of 'pure dust' in those cases where dust makes only a fractional, perhaps quite small contribution to the total AOD. This also means that the total number of profiles examined for each airport differs between CALIOP L3 and LIVAS.

Furthermore, the two approaches use different dust lidar ratios (44 sr for CALIOP L3, regionally varying for LIVAS from 40 sr in the Middle East to 56 s~~S~~r over the Western Sahara desert region ((Amiridis et al., 2013; Marinou et al., 2017; Proestakis et al., 2018; Floutsi et al., 2022), see supplement). ~~Amiridis et al. (2013) showed that the two products are not similar over the Sahara desert and Europe, with differences occurring due to both different lidar ratios and how different aerosol types are accounted for.~~

2.4 Conversion of Extinction to Mass Concentration

In order to compare the CALIPSO profiles to those from CAMS, we convert CALIPSO extinction to mass concentration according to Highwood and Ryder (2014),

$$C_{dust} = \frac{1000\sigma_e}{k_e}$$

Equation 1

where C_{dust} is the dust mass concentration (μgm^{-3}), σ_e is the extinction coefficient (km^{-1}) and k_e is the mass extinction coefficient (MEC, m^2g^{-1}), a crucial parameter in linking optical and mass-based measurements. Selection of the MEC is non-trivial since its value depends on size distribution, particle composition, shape, and may vary in time and space (Ryder et al., 2019; Ryder et al., 2018). Here, to maintain consistency with the comparison to CAMS, we apply the MEC values used within CAMS for each dust size bin (2.52, 0.94 and 0.41 m^2g^{-1} for size bins 1, 2 and 3 respectively) to the CALIOP

extinction. We calculate the vertically-varying proportion of extinction from each size bin in CAMS and then apply this weighting to the extinction in Equation 1 in order to calculate a mass concentration from CALIOP L3 and LIVAS, which thus takes into account a size-weighted MEC for each monthly mean profile. This method assumes that the size distribution represented by CAMS is the same as that sampled by CALIPSO. We choose to compare the profiles using mass, since this is the metric of interest to the aviation community, though we note that extinction comparisons showed the same results.

2.5 Dose Calculations

We calculate the dose of dust ingested by the engine core, imposed by the dusty environment in each location per flight, either for arrival (descent) or departure (ascent). Dust dose is defined as the total mass (kg) of dust ingested over a time period (different to the dosage which is the rate of dust ingestion). Dust dose is calculated from Clarkson (2020) according to:

$$dose = \int \frac{k_f w_{core} C_{dust}}{\rho_{air}} dt$$

Equation 2

where k_f is a dimensionless dust concentration/dilution factor linked with the engine regime, w_{core} is the mass flow of air entering the engine core (kg s^{-1}), C_{dust} is the ambient dust concentration (kg m^{-3}, taken from either CAMS or lidar datasets), ρ_{air} is the density of air (at a particular location, altitude and time taken from CAMS) and dt is the time integral, accounting for time spent in different engine regimes and flight phases (such as taxi, take-off) and at different altitudes. Variation of w_{core}, k_f and aircraft altitude is displayed in Figure 2 and given in the supplement.

w_{core} accounts for the operation of the engine impacting the air volume intake via effects on air flow and engine temperature: it is calculated using a mathematical model of the engine performance, matched to real engine data collected from controlled tests. The mathematical model is based on established ther~~o~~modynamics and characteristic behaviours of turbomachinery. For example, w_{core} would be lower during descent than take-off due to different engine thrust. k_f results from two effects: larger particles being entrained into the core streamtube, and the centrifuging of larger particles by the engine fan. k_f is influenced by fan blade geometry, flight speed and engine thrust as well as aerosol size distribution, and typically has values of 0.7 to 0.9 for dust or ash (Vogel et al., 2019). We use values of w_{core} and k_f as well as climb and descent rates based on a modern high bypass ratio turbofan engine provided by Clarkson (2020) and Vogel et al. (2019). Values are representative of a ~70,000 ~~lbf~~ pounds-force thrust engine, which is appropriate for a long-haul aircraft. Although values will vary for factors such as different take-off weights, day temperatures and how new the aircraft is, the maximum variation in these factors is expected to be under the order of 10%.

Dust dose is calculated at each airport for a single profile ascent or descent from each monthly mean dust profile for CAMS, CALIPSO L3 and LIVAS. Variations in time spent by the aircraft at different altitudes, engine power, dust concentration, k_f

and air density contribute to dust dose, as given by Equation 2 and height-resolved values in Figure 2. Dust dose is then averaged temporally to create a dust dose climatology. Dose is calculated separately for departure flight phases (taxi, take-off and climb) and arrival (descent, hold and approach, ground) as well as for the entire flight descent or ascent. The hold phase assumes a hold altitude of 3,000 ft (~1 km) for 10 minutes. Most holding patterns are in the 10,000 – 15,000 ft (~3 – 5 km) range, though 6,000 ft (~2 km) is not uncommon. We use 1 km for hold pattern altitude here in order to illustrate extreme exposure from dust, and test the sensitivity to hold altitude in Section 4.2.

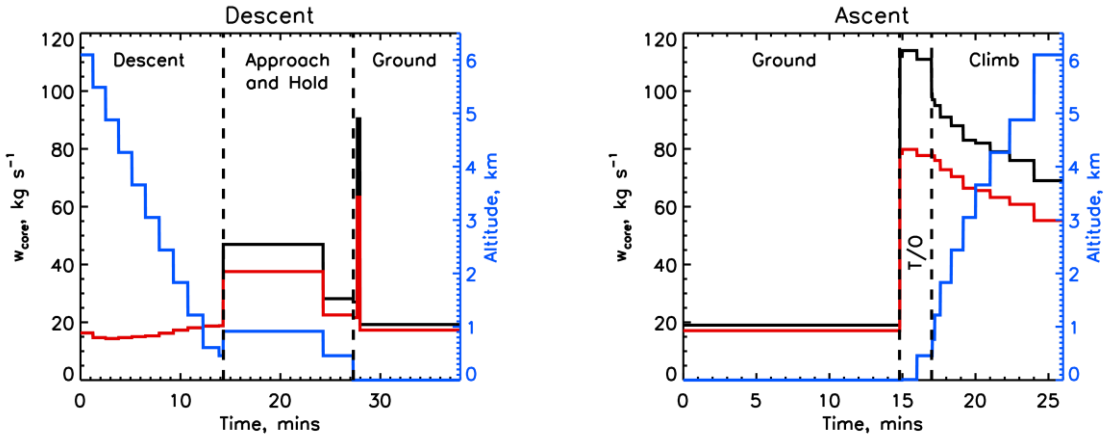

Figure 2: Variation with time of aircraft altitude (blue), w_{core} (black), and w_{core} multiplied by k_f (red line) for descent and ascent. Text and dashed black lines indicate different flight phases (T/O = take-off).

3 Results

~~3~~ In this section we present the key results and findings of this work. A full discussion of the potential causes for differences between datasets is given in Section 5.

3.1 Airport Dust Climatology

Figure 3 shows the seasonal mean dust concentration profiles for each airport using CAMS. Sydney, Phoenix, Hong Kong and Bangkok all display mean dust concentrations below 10 µgm^{-3}~~,~~, and are not discussed further. Highest concentrations are generally found in spring and summer, and are particularly notable for Niamey, Dubai, Delhi, Beijing and Marrakesh, with mean values exceeding 25 µg/m^3 in at least two seasons. During JJA dust exists in elevated layers, peaking at around 2 km for Niamey, Marrakesh, Beijing and the Canary Islands, reflecting the long-range dust transport in elevated layers occurring with transport from the Sahara desert and Gobi/Taklamakan deserts (Liu et al., 2008b; Yu et al., 2015). This contrasts to Dubai, near to dust sources, where dust peaks closer to the surface at ~200 m, with highest concentrations in JJA. Delhi shows the highest peak JJA concentration of nearly 175 µg/m^3 at around 800 m. All airports show the highest mean dust

concentrations in JJA (driven by peak solar heating and dry convection over northern hemisphere desert regions) except Beijing and Niamey. Beijing mean concentrations peak in spring at ~85 μg/m^3 at 1.5 km, driven by strong mid-latitude cyclone surface winds and low precipitation, giving rise to dust transported from the western Chinese deserts towards the Pacific Ocean (Uno et al., 2008; Han et al., 2022). The maximum concentrations in MAM at Niamey are a transition point when both elevated dust from the Sahara, as well as some contribution from low level dust driven by Harmattan winds contribute to high dust concentrations at both low and mid-altitudes. ~~Sydney, Phoenix, Hong Kong and Bangkok all display mean dust concentrations below 10 μgm^{-3}.~~

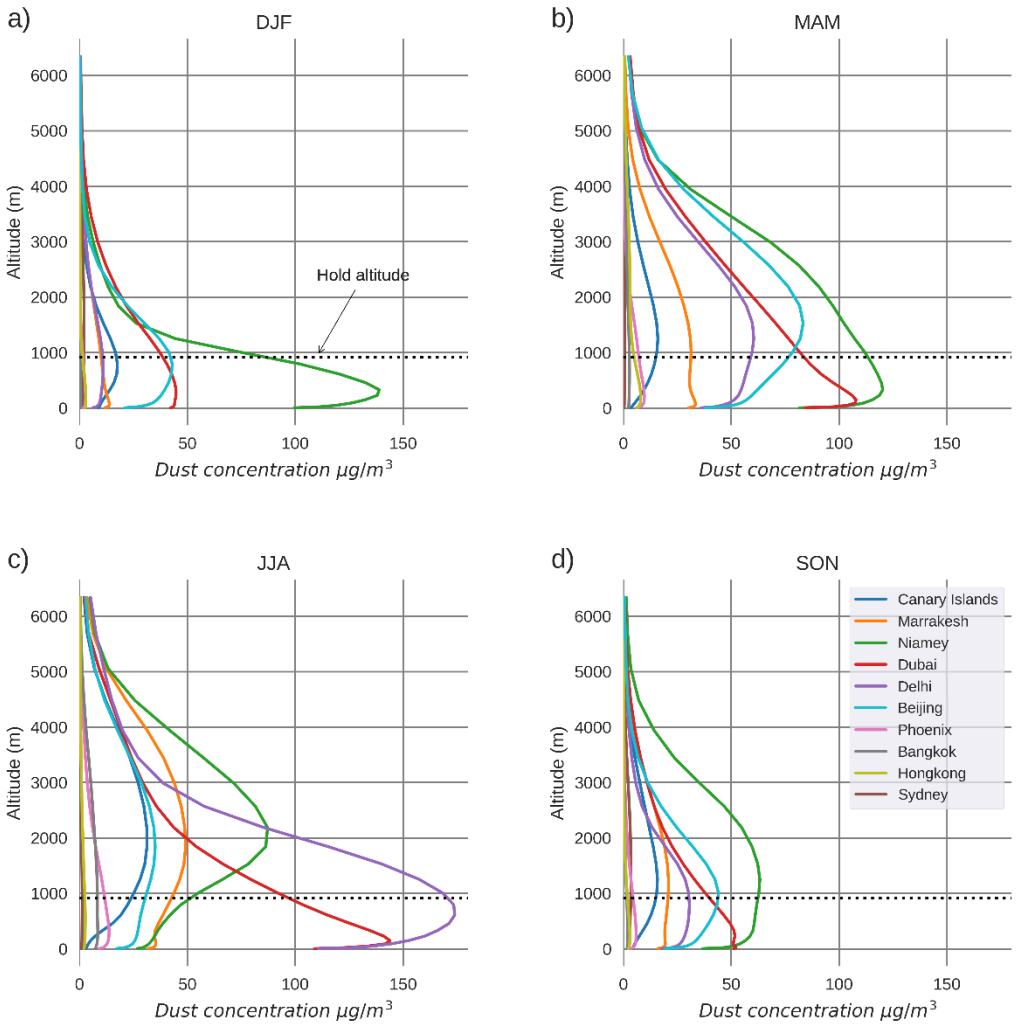

Figure 3: Seasonal mean dust concentration profiles from CAMS for 10 airports, for 2003-2019, for a) DJF; b) MAM; c) JJA and d) SON.

Figure 4 and Figure 5 show a comparison between the seasonal mean mass concentration profiles from CAMS, CALIOP L3 and LIVAS at the Canary Islands and Dubai respectively, as well as the factor difference between the lidar retrievals and CAMS. Very good agreement is found between the lidar datasets and CAMS for the Canary Islands (Figure 4), with similar vertical structure, seasonal cycle and dust concentration magnitudes, though in winter CAMS has the dust peak at a slightly more elevated altitude (1km) compared to the observations which peak closer to the surface.

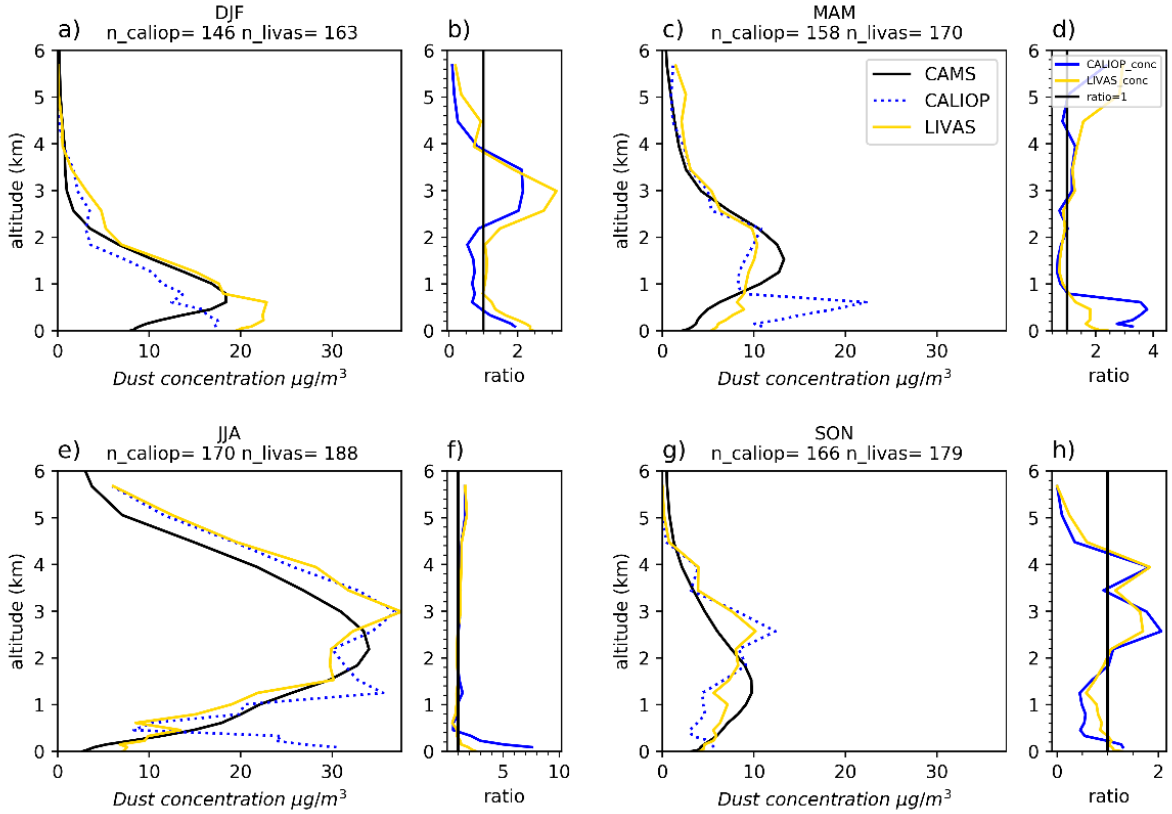

Figure 4: Canary Islands mean seasonal night-time dust concentration profiles for CAMS (black), CALIOP L3 (blue dots) and LIVAS (yellow) (a, c, e, g). Right hand column sub-figures (b, d, f, h) show the ratio of CALIOP L3 to CAMS (blue) and LIVAS to CAMS (yellow). Note that the scales of each ratio plot differ. Number of CALIOP L3 and LIVAS overpasses is given for each season. CAMS data are only included if coincident with CALIPSO data. All data cover 2007-2019.

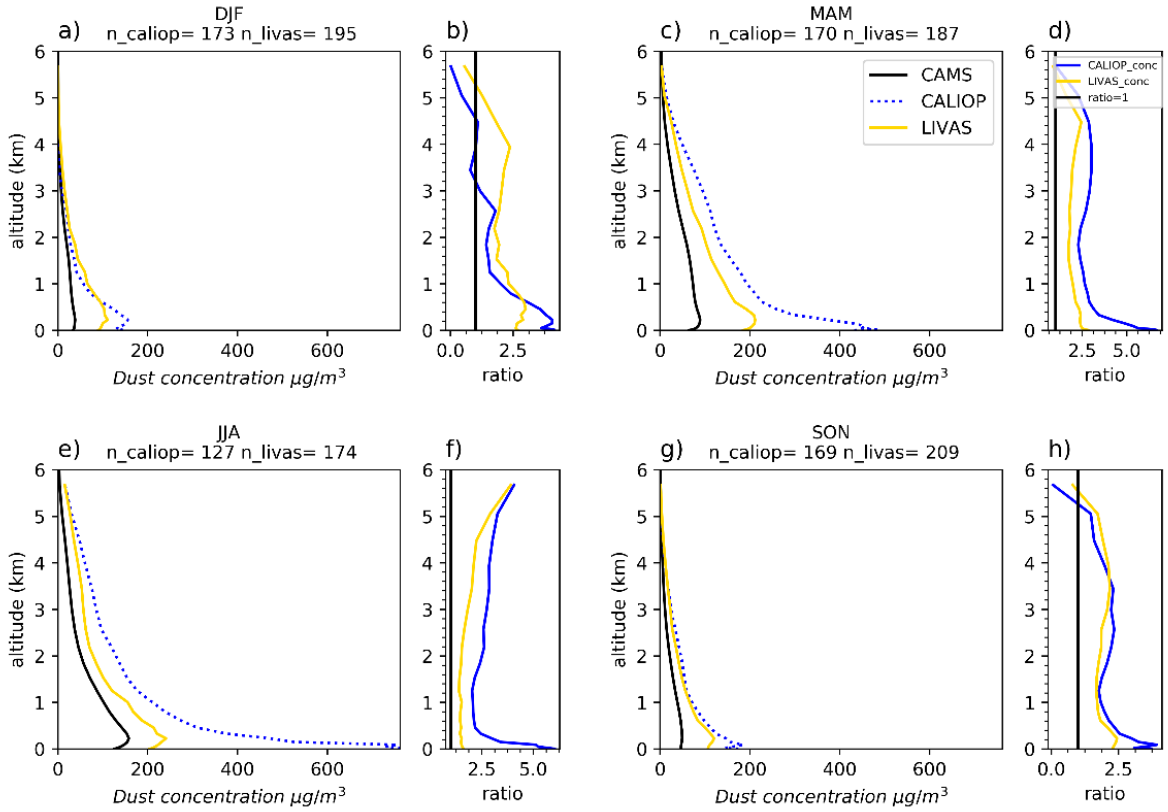

Figure 5: Same as Figure 4, except for Dubai.

At Dubai (Figure 5), CALIPSO L3 and LIVAS display the same exponential decrease in dust concentration with altitude as CAMS, and the same seasonal variations with greatest concentrations in spring and summer. However, both lidar datasets are significantly larger in magnitude than CAMS throughout the year, with CALIOP L3 exceeding a factor of 5 greater than CAMS at the lowest altitudes. LIVAS displays lower dust concentrations than CALIOP L3, but is still larger than CAMS by up to a factor of 2.5 in the lowest 1 km. Between 1 km and 5 km both lidar datasets are within a factor of 2.5 of CAMS.

Similar comparisons were performed for the other airports with significant dust loadings (see supplement). Similar to Dubai, at Niamey, Marrakesh and Delhi the shape of the vertical profile and seasonal cycles agree, though the lidar magnitudes are a factor of 2-3 greater than CAMS for Niamey and Marrakesh, but are comparable for Delhi in JJA, the peak dust season. At Beijing, although the seasonal cycles ~~were~~ are similar and dust concentrations on the same order of magnitude for CAMS and the lidar datasets, the vertical structure is very different with CAMS showing an elevated peak at around 2km while the observations show~~ed~~ an increase towards the surface. Generally LIVAS concentrations are substantially lower than CALIOP

L3, and therefore closer to concentrations from CAMS. However, in Beijing and Marrakesh dust concentrations from LIVAS are greater than CALIOP L3.

3.2 Engine core dust dose

3.2.1 CAMS

Figure 6 shows the climatological engine core dust dose calculated from CAMS for the six dustiest airports for aircraft arrival descent. Total dose (the sum of approach, hold, descent and ground doses) is highest for Delhi in JJA, at 7.56.6 g. Total dose varies by airport and season, with the highest values overall being found for Niamey, Delhi and Dubai. Delhi and Dubai encounter the greatest doses in JJA (7.56.6 g and 4.53 g), while Beijing and Niamey are greatest in MAM (2.19 g and 4.07 g), reflecting the seasonal changes in dust concentration profiles (Figure 3). Niamey stands out as the only airport with dose greater than 2 g in winter.

The greatest contribution to dose for the flight profile under consideration comes from the 'approach and hold' phase, which contributes to at least 50% of total dose in all cases. This is because the hold altitude of around 1 km frequently coincides with the altitude of peak dust concentration (Figure 3), or is very close to it. Nevertheless, the dose magnitude from approach and hold is driven by seasonal and regional variations in dust concentration. We note that hold altitude of 1 km was selected to illustrate extreme exposure that can result from low holding altitudes, and that hold patterns will not always dominate descent dust dose (Section 4.2).

The relative contributions from descent and ground phases to total arrival dose varies seasonally. For example, at Niamey there is a much greater contribution from descent to total dose in JJA when the dust plume is elevated, rather than in DJF when the contribution from the ground phase is greater due to the plume being close to the surface.

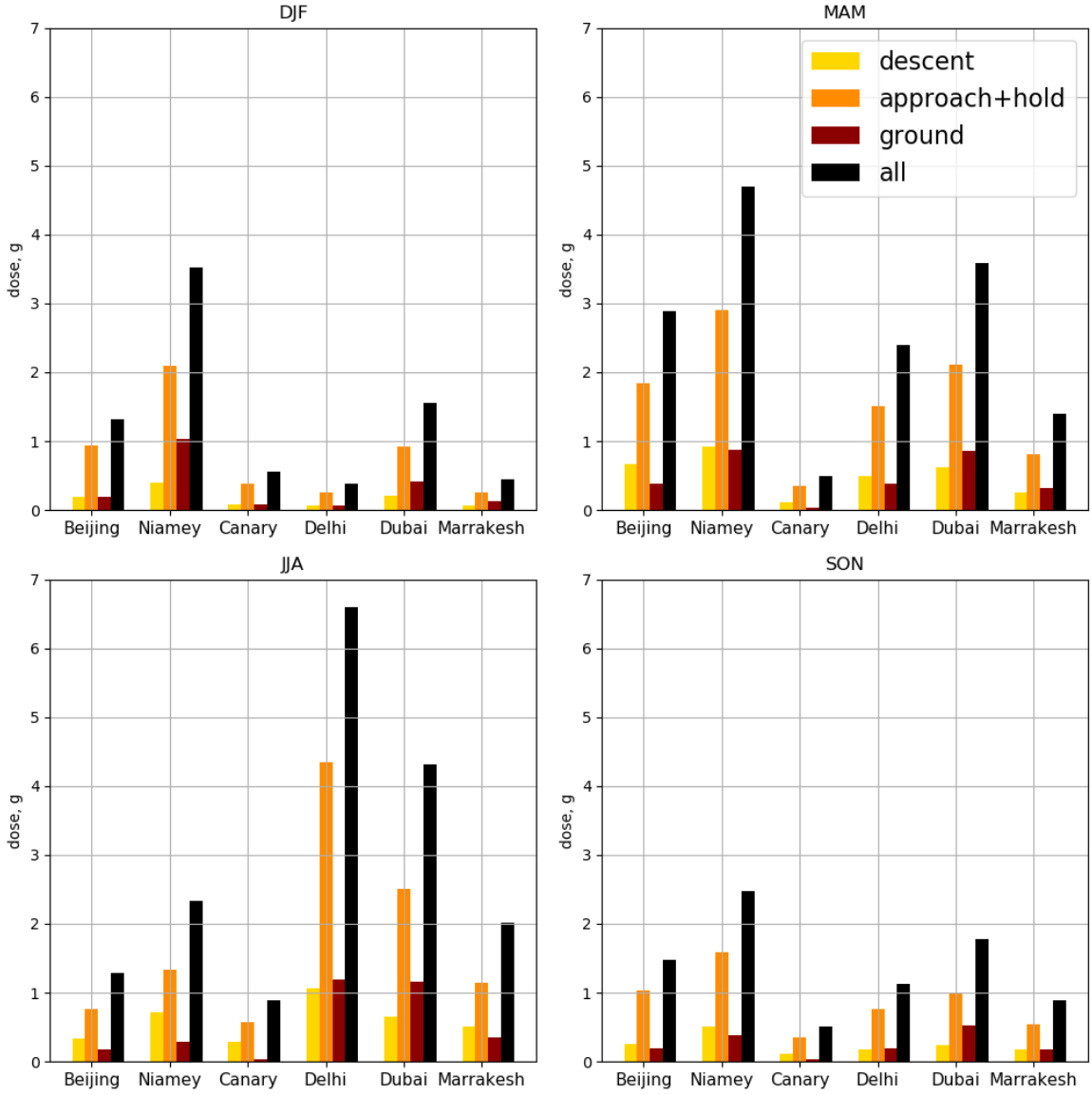

Figure 6: Climatological aircraft arrival engine core dust dose for each airport and season, separated by different flight phases and total dose. Data from CAMS covering 2003-2019.

790 For departure (Figure 7), generally total dose is slightly lower than for arrival (24% lower on average over all airports). This is due to the smaller amount of time spent departing (26 vs 38 minutes), despite significantly higher w_{core} values during departure, indicating higher engine power, as well as the lack of a holding phase which significantly contributes to arrival dose. The highest departure dose reaches a value of 4.4 g for Delhi in JJA. Similar to arrival, departure dust dose for all airports is highest in MAM and JJA, reflecting the seasonal changes in dust profiles.

795

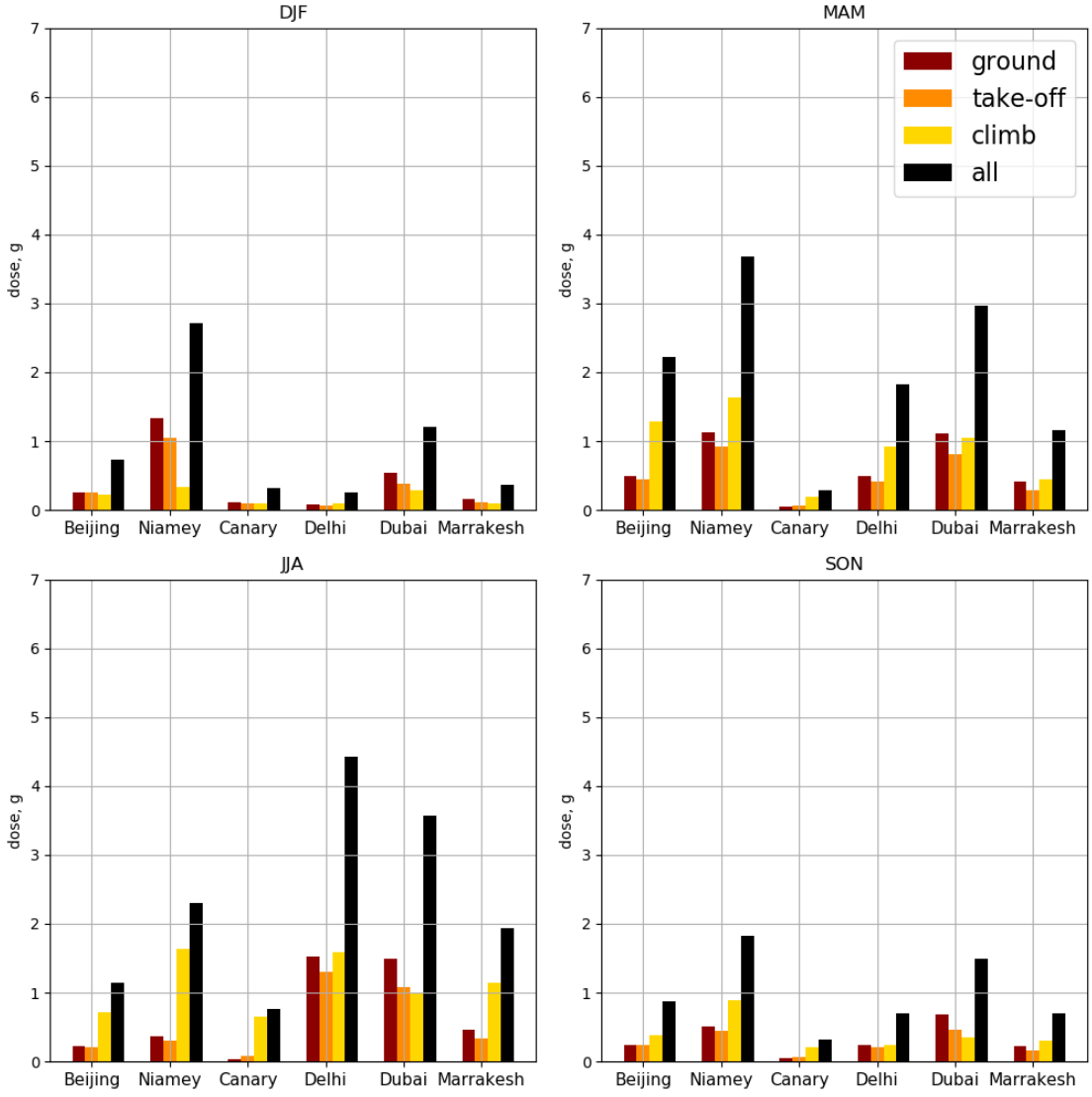

Figure 7: Climatological aircraft departure engine core dust dose for each airport and season, separated by different flight phases and total dose. Data from CAMS covering 2003-2019.

The flight phase contributing to the greatest proportion of total departure dose varies by season and airport. For airports with an elevated dust plume during MAM and JJA, such as Niamey, Beijing, Marrakesh, and the Canary Islands, the climb phase contributes the greatest proportion to total dose. Contrastingly, for airports such as Dubai and Delhi, where dust concentrations peak closer to the surface, all three flight phases contribute roughly equally to total dose. Despite the small amount of time (just over 2 minutes) spent in the take-off phase, take-off often constitutes a disproportionate second largest contribution to total dose, due to a combination of extremely high values of w_{core} and frequent coincidence with maximum or high dust concentrations.

3.2.2 CAMS vs spaceborne lidar ~~calculated~~ dose

Next we compare the dust dose calculated from CAMS to those calculated from CALIOP L3 and LIVAS data: firstly in terms of magnitude, then in terms of seasonal cycle. Figure 8 shows the magnitude of arrival dust dose ~~calculated from CAMS to those calculated from CALIOP L3 and LIVAS data~~. For certain airports such as the Canary Islands, Beijing, and to a certain extent Marrakesh, the agreement between CAMS and the lidar datasets is good - for these airports the CAMS median resides within the interquartile range of both lidar datasets.

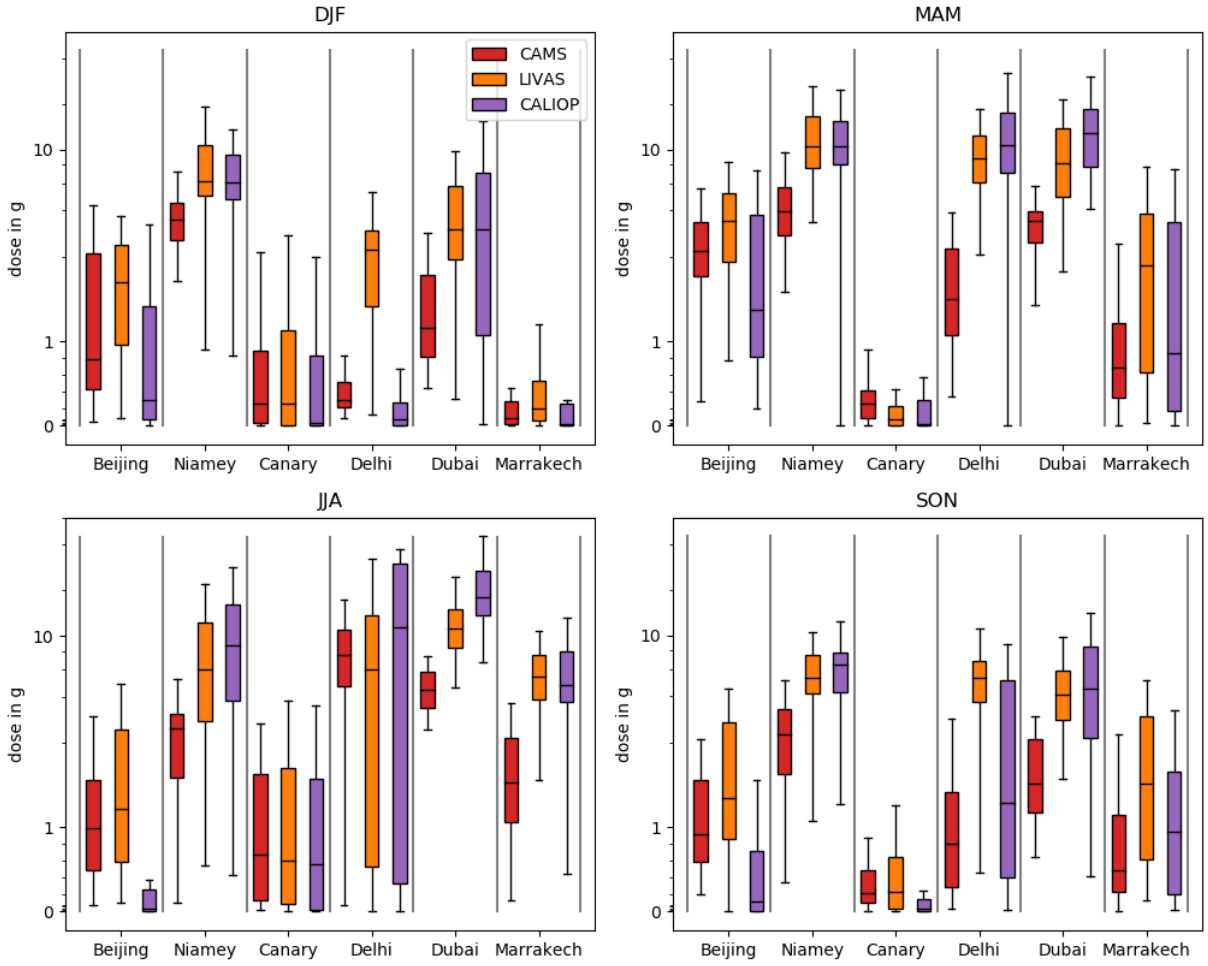

Figure 8: Seasonal engine core dust dose calculated for each airport and season for arrival, for CAMS, LIVAS and CALIOP L3 datasets. Box plots show median and interquartile range, whiskers show an additional factor of 1.5 of the interquartile range. All data cover 2007-2019. Note the semi-log scale.

The largest differences, with LIVAS and CALIOP L3 values larger than CAMS, ~~and CALIOP L3~~ and CALIOP L3 frequently larger than LIVAS~~substantially larger than both~~, are most evident at airports with a low altitude dust plume,

particularly Niamey in DJF/MAM and Dubai year-round. This is because the different datasets give very different dust concentrations close to the surface, which contributes to very different doses from the ground and hold phases, making up the largest part of descent dust dose. Differences between CALIOP L3 and LIVAS in these cases are most marked when the hold altitude mass concentrations differ. Even when the Niamey plume is elevated in JJA the doses between datasets are different (CALIOP L3 and LIVAS are a factor of 3.4 and 2.4 larger than CAMS), since the calculated dose is strongly dependent on the exact dust concentrations at the 1km holding altitude which varies between datasets, and CAMS dust concentrations are underestimated compared to the lidars at all altitudes. For Dubai, agreement is better between CAMS and LIVAS than CAMS and CALIOP L3, with CALIOP L3 median dose being 3.4 times larger than CAMS, compared to a factor of 2.6 for LIVAS. In Niamey the lidar datasets give a dose 1.7 to 3.4 times that from CAMS, though agreement between CALIOP L3 and LIVAS is much better, predominantly because dust concentrations happen to be similar at holding altitude (1 km) and at the surface, even though CALIOP L3 concentrations are around 50% larger than LIVAS in between these altitudes.

In Delhi the LIVAS dust dose is higher than both CAMS (by 6-7 times) and CALIOP L3 in DJF and SON. This is due to the dust concentration profile being larger for LIVAS than CALIOP L3 at nearly all altitudes in these seasons (see supplement). In MAM CAMS shows a much lower dose than LIVAS and CALIOP L3, while in JJA median CAMS dust doses are similar to LIVAS and CALIOP L3, though CALIOP L3 shows a larger spread.

Beijing is a second airport where the dose from LIVAS is the largest of the three datasets, a factor of 1.6 larger than CAMS. The dust concentration profiles show LIVAS to be greater than CALIOP L3 across most altitudes in all seasons, and while LIVAS shows similar magnitudes to CAMS, LIVAS profiles show a stronger surface concentration with declining concentrations in altitude, while CAMS shows a smoother profile with more elevated peaks. However, although the vertical profiles are very different, the dose calculations are fairly similar since concentrations around the holding altitude are similar, and to some extent the differences in vertical distribution compensate. CALIOP L3 shows lower doses for Beijing across all seasons, by a factor of 0.3, as a result of the smaller dust concentration profiles.

Overall there are large variations in magnitude of dose at some airports, particularly those featuring large surface concentrations and those where concentrations at holding altitude vary between the different datasets. Possible reasons behind the differences are explored in Section 5.

For departure (see supplement), overall the similarities and differences between the datasets are the same as for arrival, with lower median doses for departure by 10 to 23%, due to the lack of hold phase dose contribution during ascent. However, in a few cases doses are higher for departure than arrival. This is because differences between datasets ~~compared to arrival~~ are sensitive to the overall vertical profile shape and magnitude, particularly if ground concentrations are very large. If

concentrations are high near the ground, the extra engine power utilized during take-off, as well as the additional time spent on the ground in the taxi phase, can result in higher departure dose compared to arrival dose. For example, for Dubai in JJA, the total dose from CALIOP L3 is 18% higher for departure than arrival. This is because the departure dose is particularly sensitive to high dust concentrations at very low altitudes, and the CALIOP L3 dust concentrations in the lowest layer are nearly 4 times as large as CAMS/LIVAS. Similarly, for Beijing in MAM, greater low altitude dust concentrations from LIVAS result in a greater increase in dose from LIVAS compared to CAMS/CALIOP L3 for departure, rather than the compensation between different profile altitudes which occurs for arrival.

Other notable features are that the variability is much larger for the lidar datasets compared to CAMS, with CALIOP L3 showing slightly more variability than LIVAS. This is partly a feature of the larger magnitudes seen in the lidar data compared to CAMS, but ~~also due to the lower sampling rate for CALIPSO compared to the regular 3-hourly model output from CAMS~~and perhaps an indication that CAMS does not represent infrequent, larger dust events particularly well. Additionally, there may be differences between CALIOP L3 and LIVAS in filtering the largest, but less frequent, dust events. Section 5.2 explores this further.

Figure 9 shows the normalized seasonal cycles of dust dose in order to evaluate the seasonal timing of dust dose variability. CAMS replicates the seasonal cycles seen in the lidar data very well at Dubai, Canary Islands and Marrakech, but less well at Niamey, Beijing and Delhi. At Niamey CAMS underestimates the relative summer dust dose and overestimates the winter dose. At Beijing there is a suggestion that CAMS represents the spring peak dust dose too broadly, though the lidar datasets display disparities too. At Delhi, CAMS offsets the peak dust dose towards the late summer compared to the lidar datasets, leading to substantial differences in May and July, and also misses the secondary dust dose peak in autumn. Overall CAMS represents most of the broad seasonal variability well, but struggles to capture more detail at certain airports.

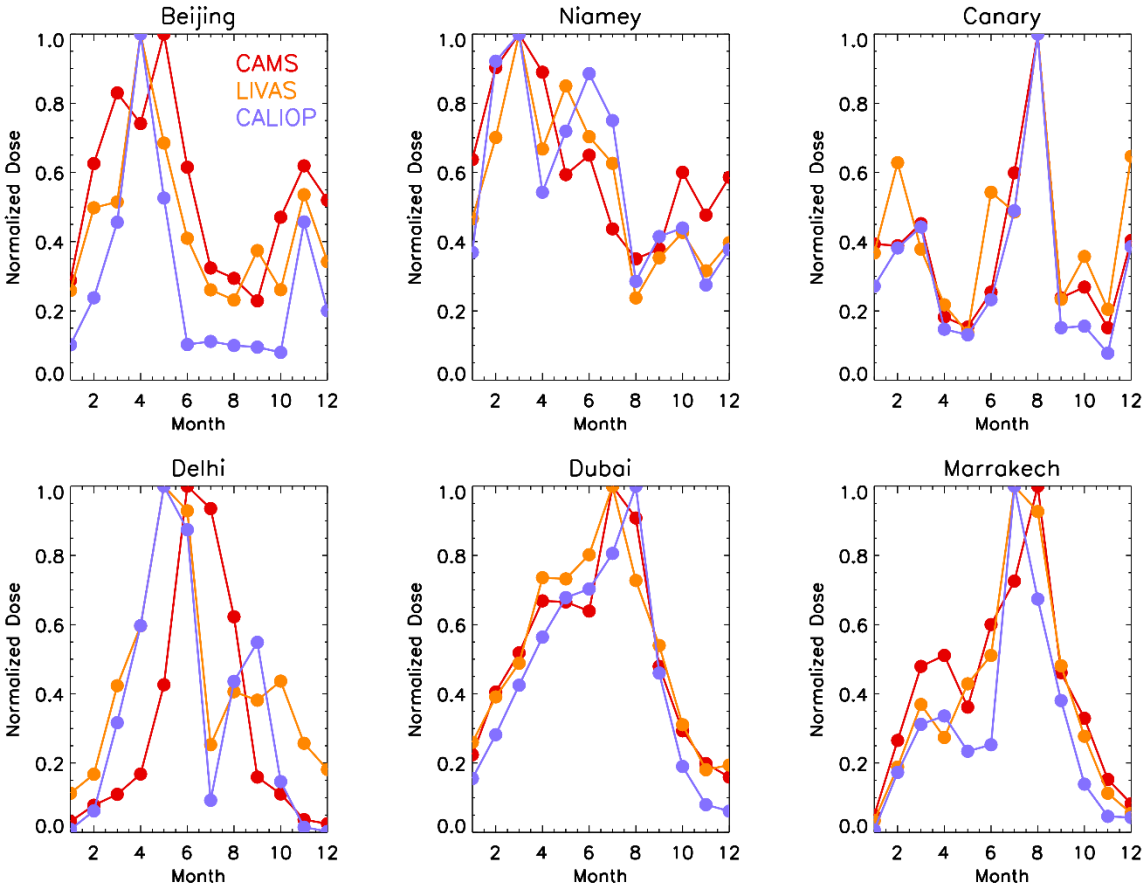

Figure 9: Seasonal variation in normalized arrival dust dose for each airport and dataset. Dose at each airport and for each dataset is normalized by the month with the largest dust dose.

4 Measures to reduce dust dose

4.1 Diurnal cycle in dose

Airports where dust is relatively local and subject to intense solar heating are subject to strong diurnal cycles in the dust concentration profile (Cuesta et al., 2009; Kocha et al., 2013). Figure 10 illustrates the CAMS mean seasonal changes in dust concentration profile at Dubai for the maximum (1600-1900 local time) during the day and the minimum during night (0100-0400 local time). During all seasons there is a strong diurnal cycle in the dust concentration, and the diurnal cycle is strongest during spring and summer. During the day, downward mixing of the nocturnal low level jet followed by intense solar heating drives local convection and dust uplift. At night time, some of this dust remains in a slightly elevated layer while surface concentrations drop due to reduced turbulent mixing of dust from the surface. This is a well-studied

phenomena impacting dust in arid regions. However, it is notable for engine ingestion purposes that night near-surface concentrations can drop to near to half of their peak day time values.

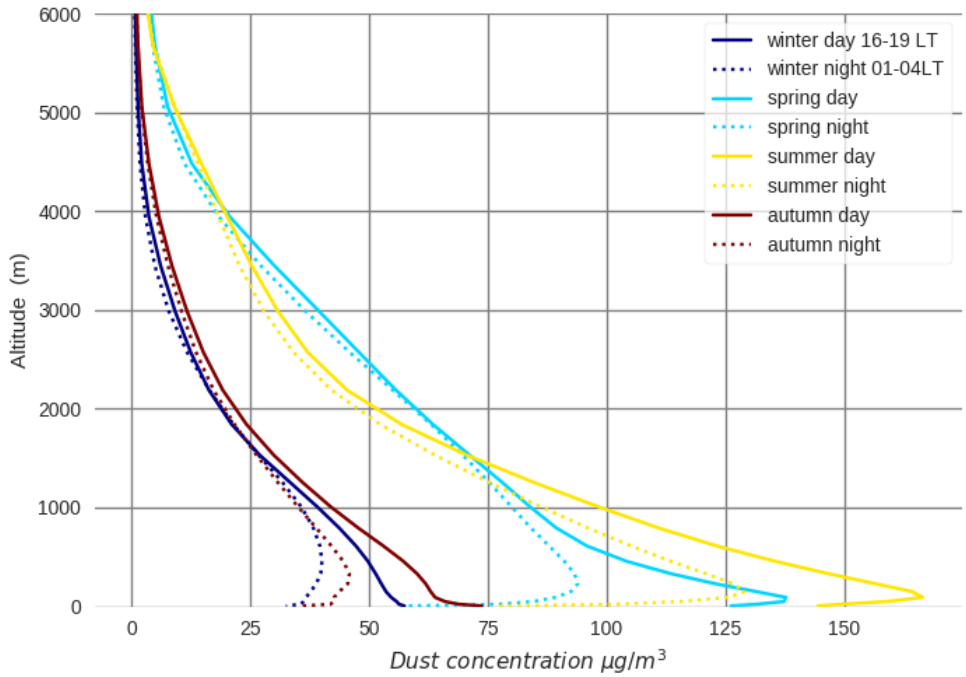

Figure 10: Diurnal cycle of dust concentration at Dubai from CAMS. Solid lines indicate daytime, dotted lines indicate night time. Day times are selected as 1600 to 1900 local time, night times as 0100 to 0400 local time.

In Table 1 we show the reduction in dust dose possible for ~~each~~ the six dustiest airports between the maximum and minimum throughout the diurnal cycle, for an arrival immediately followed by a departure, equivalent to aircraft delaying arrival and departure from late afternoon to night time. Since dust diurnal cycles are largest for profiles with high near-surface concentrations, reductions in dose due to night time flying are largest for airports with these characteristics: Dubai in JJA (5.95 g reduction), Delhi in JJA (6.44 g) and Niamey in DJF (5.00 g). For the peak dust seasons, a reduction in dose of 41% at Dubai in JJA, 34% at Delhi in JJA and 39% at Niamey in DJF could be achieved. Lower relative reductions are found at airports with ~~a~~ an elevated dust plume, such as the Canary Islands (5-194% reduction), Marrakesh (17-22% reduction) and Niamey (20% in JJA when the plume is elevated). Moderate reductions are found at Beijing (29-33 %). Substantial reductions in total dose are possible by adjusting time of day for arrival and departure.

Airport	DJF		MAM		JJA		SON	
	Dose reduction (g)	% reduction	Dose reduction (g)	% reduction	Dose reduction (g)	% reduction	Dose reduction (g)	% reduction
Beijing	1.23	33	2.219	29	1.03	29	1.328	33
Niamey	5.00	39	3.985	28	1.23	20	1.74	26
Canary Islands	0.219	14	0.218	17	0.438	19	0.105	5
Delhi	0.23	22	1.767	27	6.44	34	0.91	29
Dubai	1.84	34	4.94	39	6.05.95	41	3.108	44
Marrakesh	0.31	22	0.768	17	1.219	21	0.546	19

Table 1: Seasonal mean reduction in dust dose ~~(g)~~ between maximum and minimum throughout the diurnal cycle for an arrival directly followed by a departure for the CAMS dataset, given in g and as a percentage. Final column indicates the percentage reduction in dust dose possible for each airport's peak dust season.

4.2 Mitigation via holding altitude

The holding phase accounts for the largest proportion of dose during arrival. Therefore Figure 11 shows how selecting a different hold altitude can impact dust dose, compared to a hold altitude of 1000 m. In general dose decreases as holding altitude is raised, because for most airports dust concentration decreases with height above 1000 m. For airports such as Delhi and Dubai in JJA the changes are particularly striking, since peak dust concentrations coincide with holding altitude (Figure 3) and dust concentration drops rapidly above this altitude. Here dose from hold can be reduced by 75% (Delhi) and 63% (Dubai) by increasing hold altitude from 1 km to 3 km, equivalent to a reduction in total descent dose of 41% and 31% respectively. During spring all airport profiles exhibit broader profiles, so an increase of holding altitude to 4 km would be necessary to see substantial reductions from holding dose. Conversely, in DJF dust concentration drops off much more rapidly due to reduced boundary layer depth, providing large relative reductions from hold at 2 km.

A different pattern is shown for certain airports where an elevated dust plume is present in certain seasons, notably for Niamey in JJA where the hold dose actually increases by around 30% when holding altitude is raised to 2 km. This is also the case for the Canary Islands, Marrakesh and Beijing in JJA, though total changes in dose are much smaller (around 0.02-0.04 g), though the relative increase in hold dose can still be up to 30%. However, the vertical distribution of dust concentration from CAMS is significantly different to the lidar datasets for Beijing in MAM, JJA and SON, with CAMS indicating a dust peak at around 2km, while the lidar datasets indicate increasing concentrations towards the surface (see

supplement). This will have implications for selecting a hold altitude with the least dust dose, and a choice based on the CAMS reanalysis dataset may be inaccurate.

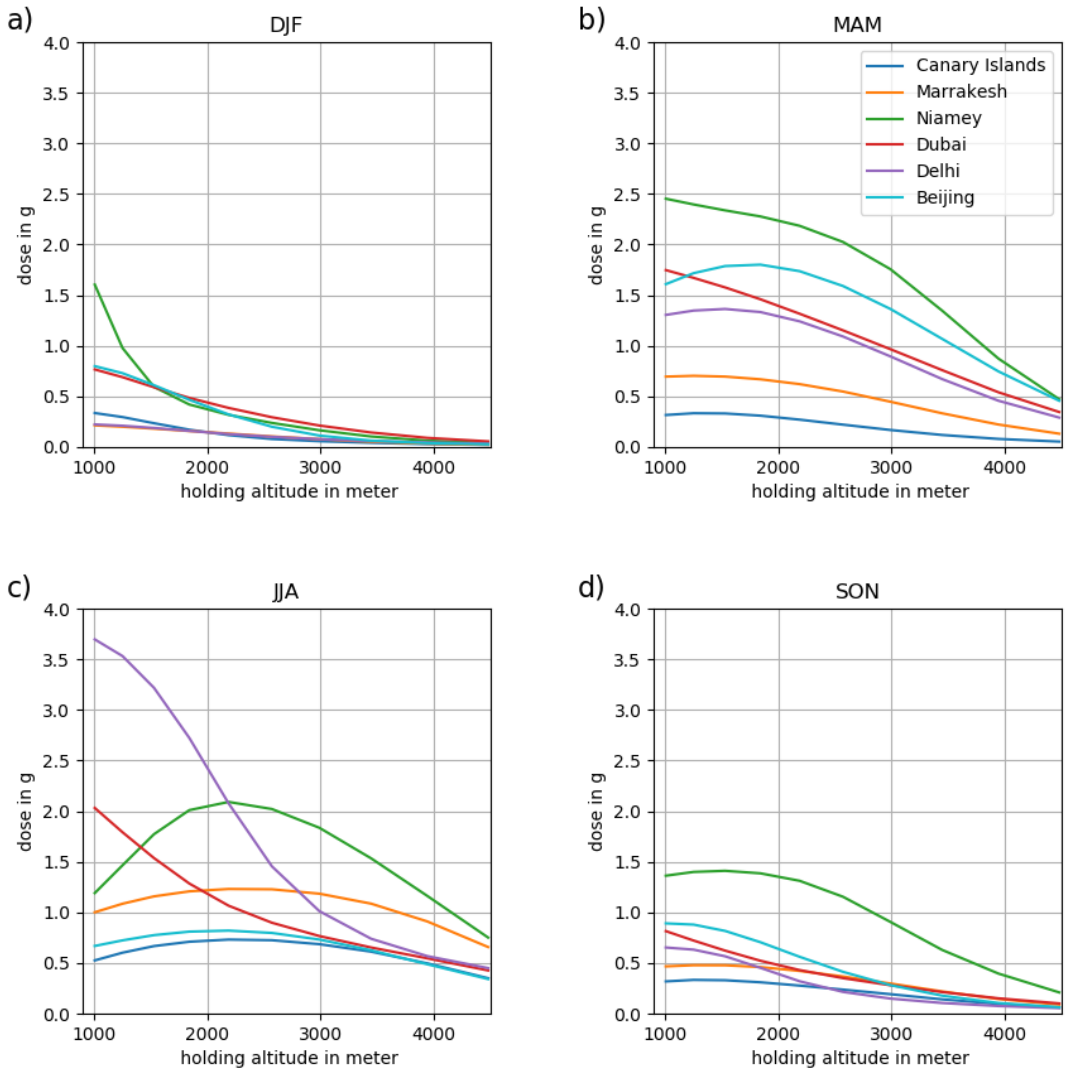

Figure 11: Dust dose (from holding pattern of 10 minutes) dependence on holding altitude from CAMS for each airport and season.

5 Discussion

Here we explore some of the causes and possible explanations for differences between the three datasets, before comparing against existing publications and discussing the implications of our findings.

5.1 CAMS vs Lidar datasets

1. The lidar profiles are filtered for clear sky (i.e., cloud-free) and have much larger grid squares over which they are averaged (2 by 5 degrees, in order to improve sampling statistics) compared to CAMS (80 km). Therefore the differences in temporal and spatial sampling introduce unquantified differences between the datasets and contribute to the differences in smoothness between CAMS and the lidar datasets.
2. Likely uncertainty in CAMS originates from the data assimilation (DA) of satellite-derived aerosol optical depth (AOD) into incorrect aerosol speciations and/or vertical distribution. For example, if the first model guess contained too little dust compared to other aerosol species, and AOD was then incremented as part of the DA process, the dust optical depth (DOD) (and therefore dust mass concentrations) would remain too low despite the assimilation of satellite aerosol retrievals. The sulfate aerosol species receives the most increments on a global scale from DA due to its ubiquity and relatively long lifetime. This may explain ~~the reason~~ why CAMS often shows too little dust compared to the lidar datasets, particularly closest to the surface, since at these altitudes total aerosol is more likely to exist as a mixture of different aerosol types. It has been noted that all aerosol reanalyses are challenged by regions with mixed dust and pollution characteristics (Xian et al., 2023). In locations more likely to contain pure dust without mixing from other aerosol types (e.g., Marrakesh and the Canary Islands), agreement between CAMS and the lidar datasets is much better.
3. Although CAMS has been shown to represent annual, spatial and seasonal variability very well for total aerosol, with good agreement with observations (Errera et al., 2021), CAMS reanalysis DOD is known to be somewhat lower than found in other datasets, such as MERRA-2 (e.g., Zhao et al. (2022); Xian et al. (2023)). The low bias of DOD over dusty regions is much more pronounced than that of total AOD, because of the issue of wrong speciation of data assimilation increments mentioned under point 2 above. Therefore we would expect comparisons against extinction or mass from lidars to be similarly low. CAMS reanalysis DOD underestimates have been shown to be on the order of around 40% compared to AERonet RObotic NETwork (AERONET) observations (Errera et al., 2021), which would roughly explain the factor of 2 or greater differences seen in this study.
4. In general, CALIOP total AOD estimates are biased low relative to other instruments (e.g. Sayer et al. (2018); Schuster et al. (2012); Song et al. (2021)). This is because CALIOP only retrieves extinction coefficients in those regions of a profile where aerosols have been detected, whereas passive sensors that cannot make height-resolved measurements necessarily retrieve optical depth estimates for the entire atmospheric column. Specific to dust, Schuster et al. (2012) found a -29% bias in CALIOP AODs in an exclusive dust environment compared to AERONET, while Song et al. (2021) found global annual mean D~~A~~OD less than a factor of two smaller than those from MODIS. Therefore it is surprising that despite this, the lidar mass profiles and doses here tend to be higher than CAMS.

5. A significant assumption is the values applied ~~for~~ to the MEC in converting between extinction and mass concentration (optical and mass parameters). If the dust composition or size distribution sampled by CALIPSO differs from that assumed or modelled in CAMS, then the conversion will be imperfect. Given a fixed composition, MEC is larger for smaller dust particles (Ryder et al., 2013; Ryder et al., 2019). Therefore in order to bring CAMS and CALIOP into better agreement, larger MEC values (representative of a greater proportion of smaller particles) would be needed to be applied to the lidar datasets. However, it has been shown that in Saharan dust plumes, CAMS may overpredict fine particles while underpredicting the coarse ones (O'sullivan et al., 2020), a common feature in dust models (Adebiyi and Kok, 2020; Adebiyi et al., 2023). The largest CAMS size bin covers a wide range of diameters (1.8 to 40 µm) with a single value of MEC. If the lowest dusty layers of the atmosphere are dominated by particles in this size range, but are more biased towards the lower end of the size range, this would justify a larger MEC at these altitudes, which would narrow the gap between the datasets.
6. CALIOP uncertainties increase nonlinearly with increasing penetration through a layer, more so where particulate concentrations are higher and for high lidar ratios (such as for dust). This frequently leads to higher uncertainties in cases where a thick dust layer is found close to the surface (e.g., Dubai year round, Niamey in DJF and MAM, Delhi in MAM, Canary Islands in DJF) (Young et al., 2013; Yu et al., 2021). High uncertainties at lower altitudes can indicate either overestimates or underestimates of the corresponding extinction coefficient. However, for the most part they tend to flag large overestimates, which may explain why airports with high surface dust concentrations show notably lower dust mass concentrations for CAMS compared to the lidar datasets.

Overall it seems most plausible that underestimates of CAMS dust mass concentrations due to the challenge of aerosol increments by DA, described in points 1-3 above are the cause of the differences between CAMS and the lidar datasets.

5.2 CALIOP L3 vs LIVAS

1. Both lidar datasets are dependent on a choice of lidar ratio to convert measured attenuated backscatter signal into extinction coefficient (44 ~~S~~sr for CALIOP L3, regionally varying for LIVAS). In reality the lidar ratio will vary spatially with dust optical properties (Schuster et al., 2012; Floutsi et al., 2022). This contributes to differences between LIVAS and CALIOP L3. For example, for Saharan dust regions where the LIVAS lidar ratio (53-56 sr) is larger than the CALIOP L3 lidar ratio it may explain the Marrakesh dust concentrations being larger in LIVAS, and possibly also Niamey. The slightly lower Middle East lidar ratio of 40 sr in LIVAS may contribute to the lower mass concentration profile in Dubai, though cannot feasibly explain the factor of 5 differences in some seasons. For the Asian airports (Beijing and Delhi) with a LIVAS lidar ratio of 46 sr, the small difference in lidar ratio compared to CALIOP L3 cannot explain the large differences in dust concentration. Therefore lidar ratio differences are not likely to be the dominant cause of differences between CALIOP L3 and LIVAS in this study.

2. CALIOP L3 and LIVAS use different depolarization thresholds for discriminating between dust and other aerosol types. CALIOP L3 uses a threshold of 0.20 while LIVAS uses 0.31. However, LIVAS also uses this threshold to extract the dusty volume from air containing a mixture of dust and other aerosol types with depolarization values between 0.05 and 0.31, which is then included in the LIVAS dust data. We did not include the 'polluted dust' or 'dusty marine' categories from CALIOP L3 since they incorporate other aerosol types besides dust, while LIVAS includes these classifications but extracts the portion of extinction within them derived from dust. Therefore, the LIVAS data includes the contribution from dust in mixed aerosol scenes while CALIOP L3 does not. These different selection approaches very likely result in different climatological profiles depending on the relative proportions of dust occurring in mixed aerosol scenes compared to the dust-only cases:
    a. When mixed aerosol type conditions occur in lower concentrations than pure dust cases, the inclusion of the dust profiles from the mixed cases in the LIVAS data will lower the mean LIVAS extinction profile compared to CALIOP L3. This occurs at low altitudes at Dubai year round, Niamey in DJF and MAM and Delhi in MAM.
    b. When mixed aerosol type conditions occur in higher concentrations than typical pure dust cases for a location, the opposite occurs, and exclusion of the dust from the mixed aerosol profiles in the CALIOP L3 data will lower the mean CALIOP L3 profile compared to LIVAS. This occurs in Beijing in all seasons and is clearest near the surface, and is also the case for Delhi in DJF and SON.

   This difference in selection and filtering of profiles most likely explains the main differences between LIVAS and CALIOP L3 found in this study. Inclusion of the mixed dust profiles from CALIOP L3 could be applied to test this hypothesis. We cannot explicitly confirm this from the analysis performed, and further exploration is beyond the scope of this article.
3. Differences are also found in the very lowest altitudes (the lowest 2 data points) between CALIOP L3 and LIVAS in cases where a very dusty profile peaks close to the surface. In these cases, CALIOP L3 concentrations drop rapidly in the lowest 2 altitude bins while LIVAS do not (Niamey DJF and MAM; Delhi JJA and MAM). This is likely to be because the lidar signal is attenuated before reaching the lowest dust layers and the dust layer base is assigned to 90 m altitude (Section 2.3.1). These cases are then excluded from CALIOP L3 data (Tackett et al., 2018). Contrastingly, we set the LIVAS data to that of the lowest altitude above where data is absent (Section 2.3.2) such that the dust concentration at these locations does not decrease rapidly towards the surface. This may result in the rapid drop-off of dust just above the surface in certain cases for CALIOP L3, though this explanation would require further investigation. Due to the importance of surface dust concentrations in determining total dose, this results in the larger CALIOP L3 dust concentrations in the overall profile at these locations being offset by the smaller CALIOP L3 surface concentrations, resulting in similar dust doses between CALIOP L3 and LIVAS in these cases.

5.3 Other Uncertainties

Finally, there are inevitably uncertainties in the quantities used to calculate w_{core} in the dust dose calculations. These mainly stem from the difference between the calibrated representative data and actual specific in-service engine and flight details. For example, the generic data assume~~s~~ a particular day temperature, humidity, airport altitude, engine condition (usually brand new) and take-off weight, all of which will vary. The largest variability in the data presented concerns whether a holding pattern was required in a flight, and the chosen altitude for the holding pattern, as explored in Section 4.2.

5.4 Comparison with Existing Dust Dose Estimations

Few published estimations of dust dose exist. Bojdo et al. (2020) used ECMWF hindcasts from CAMS to calculate engine dust dose at Doha airport for an Airbus A380-841 with Rolls-Royce Trent 900 engines, using a similar methodology to ours. They focused their study on three dusty 31 day periods (March 2017, March 2018 and 15 May to 14 June 2017) using 6 h temporal resolution. Bojdo et al. (2020) found that the average dust dose ingested into the engine core per flight was 8.5 g, with peak dust ingestion occurring just after take-off and during aircraft transition into climb phase at around 1 km. Additionally, they found that a twenty minute hold phase over the dusty Persian Gulf at around 3 km accumulated a dose of 8 g. Comparing these results to ours from Dubai (geographically closest to Doha), we find a mean dose in MAM of 3.4 g for arrival and 4.5 g for JJA for CAMS. As shown in Figure 8, the variability across our time period is around 5 g, and thus the Bojdo et al. (2020) mean value of 8.5 g falls within the boundaries of variability of our study, though falling at the higher end, likely because their values were chosen for particularly dusty periods. The Bojdo et al. (2020) hold dose calculation of 8 g is much larger than our climatological hold estimations of 2-3 g – however their value was selected as an illustration of how large holding pattern dust dose could be during the largest dust event of March 2017. Overall our findings are broadly in agreement with those of Bojdo et al. (2020), though we approach the topic from a climatological perspective, while they illustrate the likely upper end potential dust dose due to extreme conditions.

5.5 Implications of Dataset Differences

An important finding of this work is the underestimation of dust mass concentrations from CAMS relative to CALIOP, particularly evident at Dubai, Niamey, Delhi and Marrakech in certain seasons, which results in an underestimation of aircraft engine dust dose by a factor of 1.9 to 2.8. This finding has implications for general applications of the CAMS dust reanalysis, such as model validation, long-term contributions of dust to air quality targets and solar energy applications (Lacima et al., 2023; Masoom et al., 2021), but also for any stakeholders using the CAMS reanalysis for aviation purposes. Long-term calculations of engine damage using the CAMS reanalysis are likely to be underestimates, and dependent financial arrangements may be affected, such as those of overhaul providers (e.g. engine manufacturers) providing service agreements to airlines operating in dusty regions.

6 Summary and Conclusions

Atmospheric mineral dust represents a problem to aviation. There are safety considerations if dust concentrations at airports are sufficiently high that visibility drops below a few hundred metres, but this concerns the risk of collisions when manoeuvring aircraft on the ground - it is not a concern once aircraft have taken off since air traffic control keep large distances between aircraft, whatever the visibility. With regard to the direct impact dust has on aircraft, the greatest problem is the long term damage to engines from ingesting dust on the ground and flying through dusty regions which degrades engine performance and affects maintenance schedules and resource planning.

This study quantifies the climatological vertical distribution of mineral dust at a variety of worldwide airports from modelled and observed dust concentration data in order to estimate the resulting climatological core engine dust dose for the first time. We take into account typical aircraft ascent and descent rates as well as air and dust engine ingestion rates which vary with altitude, location and engine power, for a representative modern turbofan engine with a rated take-off thrust of approximately 70,000 ~~lbf~~pounds-force.

Using the ECMWF CAMS reanalysis, we find that airport dust profiles vary seasonally and regionally as expected, and that broadly, variations in engine dust dose reflect these variations. Climatologically, Sydney, Phoenix, Bangkok and Hong Kong were not very dusty, and the nature of dust damage at these airports is only likely to be occasional.

We find dust dose to be largest in JJA followed by MAM for most airports, though some airports experience different seasonal cycles: Beijing and Niamey suffered their largest dust doses in MAM, as a result of seasonal meteorological features driving dust uplift and transport. The largest arrival dose was calculated for Delhi in JJA (~~6.6~~7.5 g), followed by Niamey in MAM (4.0~~7~~ g) and Dubai in JJA (4.5~~3~~ g).

It is worth discussing the implications of a jet engine core ingesting around 5 g of mineral dust. Such a small amount of dust, on its own, represents a negligible problem for a modern jet engine core. However, when it is considered that many engines see this level of dust ingestion every flight (or ‘engine cycle’) – especially those operated by airlines with hubs of dusty airports – the cumulative dose starts to represent more of a problem; 1000 landings and subsequent departures from a dusty airport represents around 10 kg of cumulative dust ingestion. The impacts of a controlled dust ingestion test, conducted in 2018, which delivered approximately 5 kg of dust with composition representative of the region around Dubai, are reported in Elms et al. (2021). The level of contamination in the engine hot sections was enough to result in accelerated engine performance deterioration and substantially reduced component lives. Therefore the likely level of engine deterioration experienced by aircraft operating out of dusty hubs represents a significant cost to the aviation industry. Flights operating between two dusty locations, such as Delhi and Dubai, would result in double the dust ingestion.

Further, the specific type of damage caused is a function of when during the engine cycle dust is ingested. Some damage mechanisms only manifest themselves when dust is ingested at high power, such as take-off and climb. Others are driven predominantly by low power ingestion, such as idle during ground operation or during descent. Consequently, knowing how much dust is ingested during each flight phase – as quantified here – is as important as a knowledge of the total dust ingested for a complete flight.

In this study, engine dose from departure was 24% lower than that from arrival due to the large contribution to dose from the holding pattern altitude. During arrival, the hold pattern contributed over 50% of total dose due to the long time (10 minutes) spent in the hold pattern, which was compounded by hold altitude (1km) frequently occurring at, or near to, maximum dust concentrations. Contribution to dust dose from the different flight phases during departure (ground, take-off, climb) was more varied between airport and dust regime than arrival. For example, airports with seasonal elevated dust plumes (such as Beijing and Niamey in MAM and JJA and the Canary Islands and Marrakesh in JJA) experienced a dominant contribution from the higher altitude climb phase, while airports with seasonal near-surface dust plumes (e.g., Dubai year-round, Delhi in JJA) had similar contributions from all three departure flight phases.

Engine dust dose calculated from the CAMS reanalysis was compared to that from two datasets from the CALIPSO satellite with a spaceborne lidar: the standard CALIOP L3 dataset and the LIVAS dataset. Mostly the seasonal cycles in dose were very similar between CAMS and the lidar datasets, except for minor differences in the seasonal cycle at Beijing and Delhi. Likewise, CAMS mostly represented the shape of the vertical dust structure well, though CAMS tended to be unable to represent strong peaks in dust concentration near the surface seen in certain seasons at Dubai, Delhi and Niamey, and CAMS failed to represent the vertical structure ~~shape~~ at Beijing.

In terms of magnitude of dust concentration and also dust dose, values were frequently very different between all three datasets. At airports where dust was concentrated close to the surface such as Dubai, CALIOP L3 dust mass concentrations were up to 6 times greater than CAMS, and LIVAS doses up to 2.5 times greater than CAMS. Large differences in dust concentrations at low altitudes are magnified when calculating dust dose by the large contribution to total dose from the ground and hold phases. In other cases, dose calculated from LIVAS was greater than CAMS and CALIOP L3, such as at Beijing. In 46% of all seasons and airports, CAMS substantially underestimates dust dose compared to both CALIOP L3 and LIVAS, with these datasets larger by a factor of 1.9 and 2.8 respectively~~, resulting in a mean underestimate by CAMS of 2.4 over both datasets~~.

The differences in dust dose between CAMS, CALIOP L3 and LIVAS can be traced back to differences in the vertical profiles for each dataset. The comparisons are complex, firstly due to requirements for uncertain and variable properties of

dust such as the mass extinction coefficient and its contribution from different dust size ranges in converting between mass-based and optical quantities, secondly due different thresholds and methods for identifying dust in the lidar datasets, and thirdly due to challenges for both CAMS and lidar dust retrievals under conditions when dust is mixed with other aerosol types. In particular, it appears likely that CAMS underestimates dust concentrations despite the assimilation of AOD from satellites. Better observations of ~~both~~ dust properties such as size, composition, and optical properties (particularly mass extinction coefficient, which is a crucial property in relating model-calculated mass loading to satellite-derived optical retrievals) as well as more widespread comparisons between CAMS (and other dust ~~composition~~ reanalyses) and lidar vertical profiles of dust on a wider scale are required.

Finally, we examined opportunities to mitigate engine dust damage by reducing dust dose using CAMS data. Due to the diurnal cycle in dust concentration and vertical distribution, dust concentrations peak at low altitudes in the late afternoon and are at a minimum during the night. This is particularly evident in airports with low altitude dust such as Dubai, where dust dose can be reduced by up to 41% by flying at night. Many airports saw a reduction of at least 30% from night flying. Thus changing flight times could be a useful tool towards reducing dust dose. Variations in hold altitude can also significantly reduce total dose depending on the altitude of the dust maxima. Since dust generally decreases with altitude, raising hold altitude reduces dust dose. For example, at Delhi in JJA total dust dose can be reduced by 41%. However, knowledge of the dust vertical profile is crucial, since airports with elevated dust plumes can incur higher dose if holding altitude is raised into the dust plume. In this context, installation of airport-based ground lidars would be extremely useful in informing air traffic control services about the presence, concentration and altitude of dust and potential manoeuvres to avoid the highest dust concentrations. Additionally, there may be costs associated with adjusting holding altitudes and opportunities to do so will vary by airport and air traffic situations. CALIOP data were not used to investigate variation in diurnal dose due to low sampling frequency, thus these findings rely on the CAMS model reanalysis. Further investigation of the diurnal variation in vertical dust profile from observations could be probed using the Cloud-Aerosol Transport System (CATS) onboard the International Space Station (ISS) (Yorks et al., 2016), though ~~less~~ fewer than three years of data are available (Lu et al., 2023).

We note that we analyse data from the CAMS *reanalysis* here, which differs somewhat from the CAMS operational forecast, which undergoes more frequent updates and improvements. Here the use of the CAMS reanalysis was most appropriate due to its long, consistent dataset for generating a climatology of dust. Nevertheless, an evaluation of operational dust models in light of engine dust ingestion would be useful for future research, particularly since the representation of the dust life cycle in CAMS has been reviewed and improved (Remy et al., 2022). The potential use of dust forecasts operationally to adjust hold altitude for dust dose reduction could be extremely valuable.

This work provides a first quantification of aircraft engine dust dose at worldwide airports over a climatological time period. This is an increasingly important metric, given increased aircraft operations in dusty regions such as the Middle East and technological engine developments rendering them more sensitive to dust impacts. This study also provides a framework to assess the impacts of dust on aircraft engines in other contexts, such as under climate change, where although increased likelihood of drought may exacerbate dustiness (Ukkola et al., 2020; Aryal and Evans, 2021) the latest generation of climate models show a wide disparity of present day dust emissions (Zhao et al., 2022). Finally, this work emphasizes the importance of agreement between model and satellite datasets, not just in total column aerosol or dust optical depth, but for the vertical variation in dust, which is crucially important in determining aircraft engine dust dose.

7 Data availability

CAMS data are available from the Atmospheric Data Store at https://ads.atmosphere.copernicus.eu/cdsapp#!/dataset/cams-global-reanalysis-eac4?tab=overview

CALIOP L3 data are available from https://doi.org/10.5067/CALIOP/CALIPSO/CAL_LID_L3_Tropospheric_APro_cloudfree-Standard-V4-20

For the production of LIVAS dataset, CALIPSO data (provided by NASA) were obtained from the ICARE Data Center (http://www.icare.univ-lille1.fr/). The LIVAS dust products are available upon request from Vassilis Amiridis (vamoir@noa.gr), Emmanouil Proestakis (proestakis@noa.gr), and/or Eleni Marinou (elmarinou@noa.gr).

8 Author Contribution

CR, HD and RC designed the concept and experiments. CB carried out the data analysis, with guidance from CR, HD and RC. VA, EM and EP derived and provided the LIVAS data and advised on its application. SR, ZK, AB and MP advised on using the CAMS data. MV advised on application of the CALIOP data. CR prepared the manuscript, with contributions from all co-authors.

9 Competing Interests

The authors declare that they have no conflict of interest.

10 Acknowledgements

CR was funded by NERC IRF grant number NE/M018288/1. CALIOP L3 data were obtained from the NASA Langley Research Center Atmospheric Science Data Center. We thank the ICARE Data and Services Center for providing access to

the data used in this study and their computational center. EP was supported by AXA Research Fund for postdoctoral researchers under the project entitled “Earth Observation for Air-Quality – Dust Fine-Mode - EO4AQ-DustFM”.

11 References

Adebiyi, A., Kok, J. F., Murray, B. J., Ryder, C. L., Stuut, J. B. W., Kahn, R. A., Knippertz, P., Formenti, P., Mahowald, N., Garcia-Pando, C. P., Klose, M., Ansmann, A., Samset, B. H., Ito, A., Balkanski, Y., Di Biagio, C., Romanias, M. N., Huang, Y., and Meng, J.: A review of coarse mineral dust in the Earth system, Aeolian Res, 60, 10.1016/j.aeolia.2022.100849, 2023.

Adebiyi, A. A. and Kok, J. F.: Climate models miss most of the coarse dust in the atmosphere, Sci Adv, 6, 10.1126/sciadv.aaz9507, 2020.

Amiridis, V., Wandinger, U., Marinou, E., Giannakaki, E., Tsekeri, A., Basart, S., Kazadzis, S., Gkikas, A., Taylor, M., Baldasano, J., and Ansmann, A.: Optimizing CALIPSO Saharan dust retrievals, Atmos Chem Phys, 13, 12089-12106, 10.5194/acp-13-12089-2013, 2013.

Amiridis, V., Marinou, E., Tsekeri, A., Wandinger, U., Schwarz, A., Giannakaki, E., Mamouri, R., Kokkalis, P., Binietoglou, I., Solomos, S., Herekakis, T., Kazadzis, S., Gerasopoulos, E., Proestakis, E., Kottas, M., Balis, D., Papayannis, A., Kontoes, C., Kourtidis, K., Papagiannopoulos, N., Mona, L., Pappalardo, G., Le Rille, O., and Ansmann, A.: LIVAS: a 3-D multi-wavelength aerosol/cloud database based on CALIPSO and EARLINET, Atmos Chem Phys, 15, 7127-7153, 10.5194/acp-15-7127-2015, 2015.

Aryal, Y. N. and Evans, S.: Global Dust Variability Explained by Drought Sensitivity in CMIP6 Models, J Geophys Res-Earth, 126, 10.1029/2021JF006073, 2021.

Bojdo, N., Filippone, A., Parkes, B., and Clarkson, R.: Aircraft engine dust ingestion following sand storms, Aerosp Sci Technol, 106, ARTN 106072
10.1016/j.ast.2020.106072, 2020.

Bozzo, A., Benedetti, A., Flemming, J., Kipling, Z., and Remy, S.: An aerosol climatology for global models based on the tropospheric aerosol scheme in the Integrated Forecasting System of ECMWF, Geosci Model Dev, 13, 1007-1034, 10.5194/gmd-13-1007-2020, 2020.

Clarkson, R.: Atmospheric Aerosols and Gases – and How they Damage Aircraft Gas Turbine Engines, Rolls-Royce plc, 2019.

Clarkson, R.: Relating Atmospheric Contaminant Concentrations to Engine Core Dose, Rolls-Royce, UK, 2020.

Clarkson, R. J., Majewicz, E. J. E., and Mack, P.: A re-evaluation of the 2010 quantitative understanding of the effects volcanic ash has on gas turbine engines, P I Mech Eng G-J Aer, 230, 2274-2291, 10.1177/0954410015623372, 2016.

Cuesta, J., Marsham, J. H., Parker, D. J., and Flamant, C.: Dynamical mechanisms controlling the vertical redistribution of dust and the thermodynamic structure of the West Saharan atmospheric boundary layer during summer, Atmos Sci Lett, 10, 34-42, Doi 10.1002/Asl.207, 2009.

Ellis, M., Bojdo, N., Filippone, A., and Clarkson, R.: Monte Carlo Predictions of Aero-Engine Performance Degradation Due to Particle Ingestion, Aerospace-Basel, 8, ARTN 146
10.3390/aerospace8060146, 2021.

Elms, J., Pawley, A., Bojdo, N., Jones, M., and Clarkson, R.: Formation of High-Temperature Minerals From an Evaporite-Rich Dust in Gas Turbine Engine Ingestion Tests, J Turbomach, 143, 10.1115/1.4050146, 2021.

Errera, Q., Bennouna, Y., Schulz, M., Eskes, H. J., Basart, S., Benedictow, A., Blechschmidt, A. M., Chabrillat, S., Clark, H., Cuevas, E., Flentje, H., Hansen, K. M., Im, U., Kapsomenakis, J., Langerock, B., Petersen, K., Richter, A., Sudarchikova, N., Thouret, V., Wagner, A., Wang, Y., Warneke, T., and Zerefos, C.: Validation report of the CAMS global Reanalysis of aerosols and reactive gases, years 2003-2020, 10.24380/8gf9-k005, 2021.

Floutsi, A. A., Baars, H., Engelmann, R., Althausen, D., Ansmann, A., Bohlmann, S., Heese, B., Hofer, J., Kanitz, T., Haarig, M., Ohneiser, K., Radenz, M., Seifert, P., Skupin, A., Yin, Z., Abdullaev, S. F., Komppula, M., Filioglou, M., Giannakaki, E., Stachlewska, I. S., Janicka, L., Bortoli, D., Marinou, E., Amiridis, V., Gialitaki, A., Mamouri, R.-E., Barja, B., and Wandinger, U.: DeLiAn – a growing collection of depolarization ratio, lidar ratio and Ångström exponent for different aerosol types and mixtures from ground-based lidar observations, Atmospheric Measurement Technique Discussions, https://doi.org/10.5194/amt-2022-306, 2022.

Ginoux, P., Prospero, J. M., Gill, T. E., Hsu, N. C., and Zhao, M.: Global-Scale Attribution of Anthropogenic and Natural Dust Sources and Their Emission Rates Based on Modis Deep Blue Aerosol Products, Rev Geophys, 50, Artn Rg3005
10.1029/2012rg000388, 2012.

Han, Y., Wang, T. H., Tang, J. Y., Wang, C. Y., Jian, B. D., Huang, Z. W., and Huang, J. P.: New insights into the Asian dust cycle derived from CALIPSO lidar measurements, Remote Sensing of Environment, 272, 10.1016/j.rse.2022.112906, 2022.
Highwood, E. J. and Ryder, C. L.: Radiative effects of dust, in: Mineral Dust: A Key Player in the Earth System, edited by: Knippertz, P., and Stuut, J. B. W., Springer, 2014.
ICAO: European Guidance Material on All Weather Operations at Aerodromes, 2023.
Inness, A., Ades, M., Agusti-Panareda, A., Barre, J., Benedictow, A., Blechschmidt, A. M., Dominguez, J. J., Engelen, R., Eskes, H., Flemming, J., Huijnen, V., Jones, L., Kipling, Z., Massart, S., Parrington, M., Pench, V. H., Razinger, M., Remy, S., Schulz, M., and Suttie, M.: The CAMS reanalysis of atmospheric composition, Atmos Chem Phys, 19, 3515-3556, 10.5194/acp-19-3515-2019, 2019.
Kim, M. H., Omar, A. H., Tackett, J. L., Vaughan, M. A., Winker, D. M., Trepte, C. R., Hu, Y. X., Liu, Z. Y., Poole, L. R., Pitts, M. C., Kar, J., and Magill, B. E.: The CALIPSO version 4 automated aerosol classification and lidar ratio selection algorithm, Atmos Meas Tech, 11, 6107-6135, 10.5194/amt-11-6107-2018, 2018.
Knippertz, P. and Stuut, J. B. W.: Mineral Dust: A Key Player in the Earth System, 1, Springer Dordercht, https://doi.org/10.1007/978-94-017-8978-3, 2014.
Kocha, C., Tulet, P., Lafore, J. P., and Flamant, C.: The importance of the diurnal cycle of Aerosol Optical Depth in West Africa, Geophys Res Lett, 40, 785-790, 10.1002/grl.50143, 2013.
Konsta, D., Binietoglou, I., Gkikas, A., Solomos, S., Marinou, E., Proestakis, E., Basart, S., Garcia-Pando, C. P., El-Askary, H., and Amiridis, V.: Evaluation of the BSC-DREAM8b regional dust model using the 3D LIVAS-CALIPSO product, Atmos Environ, 195, 46-62, 10.1016/j.atmosenv.2018.09.047, 2018.
Lacima, A., Petetin, H., Soret, A., Bowdalo, D., Jorba, O., Chen, Z. Y., Turrubiates, R. F. M., Achebak, H., Ballester, J., and García-Pando, C. P.: Long-term evaluation of surface air pollution in CAMSRA and MERRA-2 global reanalyses over Europe (2003-2020), Geosci Model Dev, 16, 2689-2718, 10.5194/gmd-16-2689-2023, 2023.
Lee, D. S., Fahey, D. W., Skowron, A., Allen, M. R., Burkhardt, U., Chen, Q., Doherty, S. J., Freeman, S., Forster, P. M., Fuglestvedt, J., Gettelman, A., De León, R. R., Lim, L. L., Lund, M. T., Millar, R. J., Owen, B., Penner, J. E., Pitari, G., Prather, M. J., Sausen, R., and Wilcox, L. J.: The contribution of global aviation to anthropogenic climate forcing for 2000 to 2018, Atmos Environ, 244, ARTN 117834
10.1016/j.atmosenv.2020.117834, 2021.
Liu, D., Wang, Z., Liu, Z. Y., Winker, D., and Trepte, C.: A height resolved global view of dust aerosols from the first year CALIPSO lidar measurements, J Geophys Res-Atmos, 113, Artn D16214
10.1029/2007jd009776, 2008a.
Liu, Z. Y., Omar, A., Vaughan, M., Hair, J., Kittaka, C., Hu, Y. X., Powell, K., Trepte, C., Winker, D., Hostetler, C., Ferrare, R., and Pierce, R.: CALIPSO lidar observations of the optical properties of Saharan dust: A case study of long-range transport, J Geophys Res-Atmos, 113, Doi 10.1029/2007jd008878, 2008b.
Lu, Z. D., Wang, J., Chen, X., Zeng, J., Wang, Y., Xu, X. G., Christian, K. E., Yorks, J. E., Nowottnick, E. P., Reid, J. S., and Xian, P.: First Mapping of Monthly and Diurnal Climatology of Saharan Dust Layer Height Over the Atlantic Ocean From EPIC/DSCOVR in Deep Space, Geophys Res Lett, 50, ARTN e2022GL102552
10.1029/2022GL102552, 2023.
Marinou, E., Amiridis, V., Binietoglou, I., Tsikerdekis, A., Solomos, S., Proestakis, E., Konsta, D., Papagiannopoulos, N., Tsekeri, A., Vlastou, G., Zanis, P., Balis, D., Wandinger, U., and Ansmann, A.: Three-dimensional evolution of Saharan dust transport towards Europe based on a 9-year EARLINET-optimized CALIPSO dataset, Atmos Chem Phys, 17, 5893-5919, 10.5194/acp-17-5893-2017, 2017.
Masoom, A., Kosmopoulos, P., Bansal, A., Gkikas, A., Proestakis, E., Kazadzis, S., and Amiridis, V.: Forecasting dust impact on solar energy using remote sensing and modeling techniques, Sol Energy, 228, 317-332, 10.1016/j.solener.2021.09.033, 2021.
Middleton, N. J.: Desert dust hazards: A global review, Aeolian Res, 24, 53-63, 10.1016/j.aeolia.2016.12.001, 2017.
Morcrette, J. J., Beljaars, A., Benedetti, A., Jones, L., and Boucher, O.: Sea-salt and dust aerosols in the ECMWF IFS model, Geophys Res Lett, 35, Artn L24813
10.1029/2008gl036041, 2008.

Morcrette, J. J., Boucher, O., Jones, L., Salmond, D., Bechtold, P., Beljaars, A., Benedetti, A., Bonet, A., Kaiser, J. W., Razinger, M., Schulz, M., Serrar, S., Simmons, A. J., Sofiev, M., Suttie, M., Tompkins, A. M., and Untch, A.: Aerosol analysis and forecast in the European Centre for Medium-Range Weather Forecasts Integrated Forecast System: Forward modeling, J Geophys Res-Atmos, 114, Artn D06206 10.1029/2008jd011235, 2009.

Nickovic, S., Cvetkovic, B., Petkovic, S., Amiridis, V., Pejanovic, G., Solomos, S., Marinou, E., and Nikolic, J.: Cloud icing by mineral dust and impacts to aviation safety (vol 11, 6411, 2021), Sci Rep-Uk, 11, ARTN 13219 10.1038/s41598-021-92428-0, 2021.

O'Connell, J. F. and Bueno, O. E.: A study into the hub performance Emirates, Etihad Airways and Qatar Airways and their competitive position against the major European hubbing airlines, J Air Transp Manag, 69, 257-268, 10.1016/j.jairtraman.2016.11.006, 2018.

O'Sullivan, D., Marenco, F., Ryder, C. L., Pradhan, Y., Kipling, Z., Johnson, B., Benedetti, A., Brooks, M., McGill, M., Yorks, J., and Selmer, P.: Models transport Saharan dust too low in the atmosphere: a comparison of the MetUM and CAMS forecasts with observations, Atmos Chem Phys, 20, 12955-12982, 10.5194/acp-20-12955-2020, 2020.

Papagiannopoulos, N., D'Amico, G., Gialitaki, A., Ajtai, N., Alados-Arboledas, L., Amodeo, A., Amiridis, V., Baars, H., Balis, D., Binietoglou, I., Comeron, A., Dionisi, D., Falconieri, A., Freville, P., Kampouri, A., Mattis, I., Mijic, Z., Molero, F., Papayannis, A., Pappalardo, G., Rodriguez-Gomez, A., Solomos, S., and Mona, L.: An EARLINET early warning system for atmospheric aerosol aviation hazards, Atmos Chem Phys, 20, 10775-10789, 10.5194/acp-20-10775-2020, 2020.

Pappalardo, G., Amodeo, A., Apituley, A., Comeron, A., Freudenthaler, V., Linne, H., Ansmann, A., Bosenberg, J., D'Amico, G., Mattis, I., Mona, L., Wandinger, U., Amiridis, V., Alados-Arboledas, L., Nicolae, D., and Wiegner, M.: EARLINET: towards an advanced sustainable European aerosol lidar network, Atmos Meas Tech, 7, 2389-2409, 10.5194/amt-7-2389-2014, 2014.

Prata, A. and Rose, W. I.: Volcanic ash hazards to aviation, in: The Encyclopedia of Volcanoes, edited by: Sigurdssonm, H., Houghton, B., McNutt, S., Rymer, H., and Stix, J., Elsevier, 911-934, 2015.

Prata, A. J., Kristiansen, N., Thomas, H. E., and Stohl, A.: Ash Metrics for European and Trans-Atlantic Air Routes During the Eyjafjallajokull Eruption 14 April to 23 May 2010, J Geophys Res-Atmos, 123, 5469-5483, 10.1002/2017jd028199, 2018.

Proestakis, E., Amiridis, V., Marinou, E., Georgoulias, A. K., Solomos, S., Kazadzis, S., Chimot, J., Che, H. Z., Alexandri, G., Binietoglou, I., Daskalopoulou, V., Kourtidis, K. A., de Leeuw, G., and Ronald, J. V.: Nine-year spatial and temporal evolution of desert dust aerosols over South and East Asia as revealed by CALIOP, Atmos Chem Phys, 18, 1337-1362, 10.5194/acp-18-1337-2018, 2018.

Prospero, J. M., Ginoux, P., Torres, O., Nicholson, S. E., and Gill, T. E.: Environmental characterization of global sources of atmospheric soil dust identified with the Nimbus 7 Total Ozone Mapping Spectrometer (TOMS) absorbing aerosol product, Rev Geophys, 40, Artn 1002 10.1029/2000rg000095, 2002.

Remy, S., Kipling, Z., Huijnen, V., Flemming, J., Nabat, P., Michou, M., Ades, M., Engelen, R., and Peuch, V. H.: Description and evaluation of the tropospheric aerosol scheme in the Integrated Forecasting System (IFS-AER, cycle 47R1) of ECMWF, Geosci Model Dev, 15, 4881-4912, 10.5194/gmd-15-4881-2022, 2022.

Rémy, S., Kipling, Z., Flemming, J., Boucher, O., Nabat, P., Michou, M., Bozzo, A., Ades, M., Huijnen, V., Benedetti, A., Engelen, R. J., Peuch, V. H., and Morcrette, J. J.: Description and evaluation of the tropospheric aerosol scheme in the European Centre for Medium-Range Weather Forecasts (ECMWF) Integrated Forecasting System (IFS-AER, cycle 45R1), Geosci Model Dev, 12, 4627-4659, 10.5194/gmd-12-4627-2019, 2019.

Ryder, C. L., Highwood, E. J., Walser, A., Seibert, P., Philipp, A., and Weinzierl, B.: Coarse and giant particles are ubiquitous in Saharan dust export regions and are radiatively significant over the Sahara, Atmos Chem Phys, 19, 15353-15376, 10.5194/acp-19-15353-2019, 2019.

Ryder, C. L., Highwood, E. J., Rosenberg, P. D., Trembath, J., Brooke, J. K., Bart, M., Dean, A., Crosier, J., Dorsey, J., Brindley, H., Banks, J., Marsham, J. H., McQuaid, J. B., Sodemann, H., and Washington, R.: Optical properties of Saharan dust aerosol and contribution from the coarse mode as measured during the Fennec 2011 aircraft campaign, Atmos Chem Phys, 13, 303-325, DOI 10.5194/acp-13-303-2013, 2013.

Ryder, C. L., Marenco, F., Brooke, J. K., Estelles, V., Cotton, R., Formenti, P., McQuaid, J. B., Price, H. C., Liu, D. T., Ausset, P., Rosenberg, P. D., Taylor, J. W., Choularton, T., Bower, K., Coe, H., Gallagher, M., Crosier, J., Lloyd, G., Highwood, E. J., and Murray, B. J.: Coarse-mode mineral dust size distributions, composition and optical properties from AER-D aircraft measurements over the tropical eastern Atlantic, Atmos Chem Phys, 18, 17225-17257, 10.5194/acp-18-17225-2018, 2018.

Sayer, A. M., Hsu, N. C., Lee, J., Kim, W. V., Dubovik, O., Dutcher, S., Huang, D., Litvinov, P., Lyapustin, A., Tackett, J. L., and Winker, D. M.: Validation of SOAR VIIRS Over-Water Aerosol Retrievals and Context Within the Global Satellite Aerosol Data Record, J Geophys Res-Atmos, 123, 13496-13526, 10.1029/2018jd029465, 2018.

Schuster, G. L., Vaughan, M., MacDonnell, D., Su, W., Winker, D., Dubovik, O., Lapyonok, T., and Trepte, C.: Comparison of CALIPSO aerosol optical depth retrievals to AERONET measurements, and a climatology for the lidar ratio of dust, Atmos Chem Phys, 12, 7431-7452, 10.5194/acp-12-7431-2012, 2012.

Song, Q. Q., Zhang, Z. B., Yu, H. B., Ginoux, P., and Shen, J.: Global dust optical depth climatology derived from CALIOP and MODIS aerosol retrievals on decadal timescales: regional and interannual variability, Atmos Chem Phys, 21, 13369-13395, 10.5194/acp-21-13369-2021, 2021.

Tackett, J. L., Winker, D. M., Getzewich, B. J., Vaughan, M. A., Young, S. A., and Kar, J.: CALIPSO lidar level 3 aerosol profile product: version 3 algorithm design, Atmos Meas Tech, 11, 4129-4152, 10.5194/amt-11-4129-2018, 2018.

Tesche, M., Ansmann, A., Muller, D., Althausen, D., Engelmann, R., Freudenthaler, V., and Gross, S.: Vertically resolved separation of dust and smoke over Cape Verde using multiwavelength Raman and polarization lidars during Saharan Mineral Dust Experiment 2008, J Geophys Res-Atmos, 114, 10.1029/2009jd011862, 2009.

Ukkola, A. M., De Kauwe, M. G., Roderick, M. L., Abramowitz, G., and Pitman, A. J.: Robust Future Changes in Meteorological Drought in CMIP6 Projections Despite Uncertainty in Precipitation, Geophys Res Lett, 47, 10.1029/2020GL087820, 2020.

Uno, I., Yumimoto, K., Shimizu, A., Hara, Y., Sugimoto, N., Wang, Z., Liu, Z., and Winker, D. M.: 3D structure of Asian dust transport revealed by CALIPSO lidar and a 4DVAR dust model, Geophys Res Lett, 35, 10.1029/2007gl032329, 2008.

Vogel, A., Durant, A. J., Cassiani, M., Clarkson, R. J., Slaby, M., Diplas, S., Kruger, K., and Stohl, A.: Simulation of Volcanic Ash Ingestion Into a Large Aero Engine: Particle-Fan Interactions, J Turbomach, 141, 10.1115/1.4041464, 2019.

Winker, D. M., Hunt, W. H., and McGill, M. J.: Initial performance assessment of CALIOP, Geophys Res Lett, 34, Artn L19803
10.1029/2007gl030135, 2007.

Winker, D. M., Pelon, J., Coakley, J. A., Ackerman, S. A., Charlson, R. J., Colarco, P. R., Flamant, P., Fu, Q., Hoff, R. M., Kittaka, C., Kubar, T. L., Le Treut, H., McCormick, M. P., Megie, G., Poole, L., Powell, K., Trepte, C., Vaughan, M. A., and Wielicki, B. A.: THE CALIPSO MISSION A Global 3D View of Aerosols and Clouds, B Am Meteorol Soc, 91, 1211-1229, 10.1175/2010bams3009.1, 2010.

Xian, P., Reid, J. S., Ades, M., Benedetti, A., Colarco, P., da Silva, A., Eck, T., Flemming, J., Hyer, E. J., Kipling, Z., Remy, S., Sekiyama, T., Tanaka, T. Y., Yumimoto, K., and Zhang, J.: Intercomparison of Aerosol Optical Depths from four reanalyses and their multi-reanalysis-consensus, EGUsphere Preprint, https://doi.org/10.5194/egusphere-2023-2354, 2023.

Yang, W. D., Marshak, A., Kostinski, A. B., and Varnai, T.: Shape-induced gravitational sorting of Saharan dust during transatlantic voyage: Evidence from CALIOP lidar depolarization measurements, Geophys Res Lett, 40, 3281-3286, 10.1002/grl.50603, 2013.

Yorks, J. E., McGill, M. J., Palm, S. P., Hlavka, D. L., Selmer, P. A., Nowottnick, E. P., Vaughan, M. A., Rodier, S. D., and Hart, W. D.: An overview of the CATS level 1 processing algorithms and data products, Geophys Res Lett, 43, 4632-4639, 10.1002/2016gl068006, 2016.

Young, S. A., Vaughan, M. A., Kuehn, R. E., and Winker, D. M.: The Retrieval of Profiles of Particulate Extinction from Cloud-Aerosol Lidar and Infrared Pathfinder Satellite Observations (CALIPSO) Data: Uncertainty and Error Sensitivity Analyses, J Atmos Ocean Tech, 30, 395-428, 10.1175/Jtech-D-12-00046.1, 2013.

Young, S. A., Vaughan, M. A., Garnier, A., Tackett, J. L., Lambeth, J. D., and Powell, K. A.: Extinction and optical depth retrievals for CALIPSO's Version 4 data release, Atmos Meas Tech, 11, 5701-5727, 10.5194/amt-11-5701-2018, 2018.

Yu, H., Tan, Q., Zhou, L., Bian, H. S., Chin, M., Ryder, C. L., Levy, R., Pradhan, Y., Shi, Y., Song, Q., Zhang, Z., Colarco, P., Kim, D., Remer, L., Yuan, T., Mayol-Bracero, O. L., and Holben, B.: Observation and modeling of a gigantic African

dust intrusion into the Caribbean Basin and the southern U.S. in June 2020, Atmos. Chem. Phys., 21, 12359–12383, 10.5194/acp-21-12359-2021, 2021.
Yu, H. B., Chin, M., Bian, H. S., Yuan, T. L., Prospero, J. M., Omar, A. H., Remer, L. A., Winker, D. M., Yang, Y. K., Zhang, Y., and Zhang, Z. B.: Quantification of trans-Atlantic dust transport from seven-year (2007-2013) record of CALIPSO lidar measurements, Remote Sensing of Environment, 159, 232-249, 10.1016/j.rse.2014.12.010, 2015.
Zhao, A., Ryder, C. L., and Wilcox, L. J.: How well do the CMIP6 models simulate dust aerosols?, Atmos Chem Phys, 22, 2095-2119, 10.5194/acp-22-2095-2022, 2022.